Corticosteroids compromise survival in glioblastoma

Pitter, K L ; Tamagno, I ; Alikhanyan, K ; Hosni-Ahmed, A ; Pattwell, S S ; Donnola, S ; Dai, C ; Ozawa, T ; Chang, M ; Chan, T A ; Beal, K ; Bishop, A J ; Barker, C A ; Jones, T S ; Hentschel, B ; Gorlia, T ; Schlegel, U ; Stupp, R ; Weller, M ; Holland, E C ; Hambardzumyan, D

Abstract: Glioblastoma is the most common and most aggressive primary brain tumour. Standard of care consists of surgical resection followed by radiotherapy and concomitant and maintenance temozolomide (temozolomide/radiotherapy→temozolomide). Corticosteroids are commonly used perioperatively to control cerebral oedema and are frequently continued throughout subsequent treatment, notably radiotherapy, for amelioration of side effects. The effects of corticosteroids such as dexamethasone on cell growth in glioma models and on patient survival have remained controversial. We performed a retrospective analysis of glioblastoma patient cohorts to determine the prognostic role of steroid administration. A disease-relevant mouse model of glioblastoma was used to characterize the effects of dexamethasone on tumour cell proliferation and death, and to identify gene signatures associated with these effects. A murine anti-VEGFA antibody was used in parallel as an alternative for oedema control. We applied the dexamethasone-induced gene signature to The Cancer Genome Atlas glioblastoma dataset to explore the association of dexamethasone exposure with outcome. Mouse experiments were used to validate the effects of dexamethasone on survival in vivo Retrospective clinical analyses identified corticosteroid use during radiotherapy as an independent indicator of shorter survival in three independent patient cohorts. A dexamethasone-associated gene expression signature correlated with shorter survival in The Cancer Genome Atlas patient dataset. In glioma-bearing mice, dexamethasone pretreatment decreased tumour cell proliferation without affecting tumour cell viability, but reduced survival when combined with radiotherapy. Conversely, anti-VEGFA antibody decreased proliferation and increased tumour cell death, but did not affect survival when combined with radiotherapy. Clinical and mouse experimental data suggest that corticosteroids may decrease the effectiveness of treatment and shorten survival in glioblastoma. Dexamethasone-induced anti-proliferative effects may confer protection from radiotherapy- and chemotherapy-induced genotoxic stress. This study highlights the importance of identifying alternative agents such as vascular endothelial growth factor antagonists for managing oedema in glioblastoma patients. Beyond the established adverse effect profile of protracted corticosteroid use, this analysis substantiates the request for prudent and restricted use of corticosteroids in glioblastoma.

DOI: https://doi.org/10.1093/brain/aww046

Pitter, K L; Tamagno, I; Alikhanyan, K; Hosni-Ahmed, A; Pattwell, S S; Donnola, S; Dai, C; Ozawa, T; Chang, M; Chan, T A; Beal, K; Bishop, A J; Barker, C A; Jones, T S; Hentschel, B; Gorlia, T; Schlegel, U; Stupp, R; Weller, M; Holland, E C; Hambardzumyan, D (2016). Corticosteroids compromise survival in glioblastoma. Brain, 139(Pt 5):1458-1471.
DOI: https://doi.org/10.1093/brain/aww046

1/6/15

Dimitri Michael Kullmann, MD, PhD; Editor-in-Chief
Brain

Dear Dr. Kullmann,

Please find enclosed our revised manuscript entitled "**CORTICOSTEROIDS COMPROMISE SURVIVAL IN GLIOBLASTOMA"** for consideration to be published as a research article in *Brain.* We appreciate the advice and comments provided by the reviewers and editor.

We have attached a detailed list of changes we have made in manuscript, and point-by-point responses to the referees' and editor's concerns. By addressing the majority of these points, and incorporating their suggestions in the text of manuscript, we feel that the paper is now considerably stronger.

This work represents a major breakthrough in our understanding of glioblastoma clinical management. Currently the majority of glioblastoma patients receive corticosteroids during radiation. However, our work suggests that this standard of care is counterproductive and alternatives to corticosteroids during radiation should be developed. This paper is the most extensive work published on this topic and includes modeling and mechanistic studies. It is likely to be highly cited as the standard of care for this disease is adjusted."

The manuscript contains 8 figures, total of 8 supplementary figures and tables. All authors have read and approved the final version of the manuscript. We feel that this work will be of broad interest to the readers of *Brain* because it identifies DEX use during radiotherapy as an independent indicator of shorter survival and proposes alternative anti-edema therapy that does not compromise radiation efficacy.

Thank you for your careful consideration of our work.

Sincerely yours,

Dolores Hambardzumyan, PhD
Eric C Holland, MD, PhD
Michael Weller, MD, PhD

MAJOR POINTS

COMMENT: The authors show that application of high doses of DEX to GBM-patients is associated with an inferior clinical outcome; they also discuss that higher concentrations of DEX are generally given to patients with inferior clinical perspective. Hence, larger sets of patients were statistically analysed to separate DEX-mediated detrimental effects from other clinical aspects (extent of resection, age, neurological symptoms and radiation dose). In some

retrospective analyses (but not in all studies) DEX was an independent adverse factor. Due to the difficulties to assess the role of DEX from clinical samples alone the animal experiments are highly important to support the working hypothesis that DEX indeed is causative for reduced overall survival. However, the animal model reflects basically one GBM subtype (proneural GBM), which can differ in terms of radiation- and chemo-sensitivity from other GBM-subtypes. Therefore it will be important to see if the statistical analysis of clinical trials still holds, when the effects of DEX are studied in cohorts of patients with proneural GBM.

RESPONSE: We do appreciate the reviewer's suggestion, but unfortunately we do not have the information on the Verhaak subtypes in any of these cohorts.

COMMENT: The authors explain the adverse effect of DEX-application by the reduced radio-sensitivity of glioma cells: it is speculated that GBM cells have reduced proliferativity (and therefore potentially reduced radiosensitivity) after DEX-application. This view is partly supported by data from an expression array showing that a (relatively small) number of cell-cycle regulatory genes is down-modulated in gliomas from DEX-treated mouse models, as compared to controls. This is likely to be over-simplistic and other, parenchymal effects of DEX-treatment need to be taken into consideration: DEX blunts the immune response but immune effects were not investigated. It is necessary to study the number of tumour associated myeloid cells and angiogenesis in DEX-treated glioma bearing mice, as already done for B20-treated models. All potential effects of DEX on the vasculature were not addressed - although the main reason for DEX treatment is edema-relief. It is necessary to study the number of tumour associated myeloid cells and angiogenesis in DEX-treated glioma bearing mice, as already done for B20-treated models. This is especially important since in vitro experiments did not show any effects of radiation-treatment in glioma cell-cycle progression.

***RESPONSE**: We are thankful for these suggestions and we do agree with reviewer about the complexity of DEX effects in vivo and the importance of looking at stromal effects of DEX since we did not see difference in DEX effects on proliferation in vitro.*

Per reviewer's suggestion we have looked at the numbers of infiltrated tumor-associated microglia/macrophages (myeloid cells) in response to either DEX or VEGFA antibody treatment. Microglia/macrophages are the major immune infiltrates in both murine and human glioblastoma. Others and we have previously demonstrated that microglia/macrophages can contribute up to 20-30 % of the total tumor mass (Feng et al., 2015; Hambardzumyan et al., 2015). While we saw a significant increase in Iba1 positive microglia/macrophage infiltration in B20-4.1.1 treated mice when compared to vehicle, no difference was observed between DEX-treated and vehicle treated tumors in our treatment paradigm ***(incorporated as a new Supplemental Fig. 3C**).*

To address the role of DEX in edema relief in our mouse model, we developed a novel T2 weighted MRI assay described below. To our surprise we were unable to find studies looking at the edema effects of DEX using mouse models of brain tumors. Unfortunately it was not feasible to directly measure edema in the mouse model using techniques such as MRI-FLAIR. Rather, we

*developed an alternative strategy using T2 MRI based on the principle that decreasing edema would allow glioma-bearing mice to survive with larger tumor volumes compared to vehicle treated animals. Therefore, one would expect untreated animals would develop symptoms of increased intracranial pressure with a smaller tumor volume than DEX or B20-4.1.1 treated animals. To address this, we evenly distributed animals into vehicle or DEX treated cohorts based on initial T2-weight MRI tumor volume to ensure equal distribution of baseline tumor volumes. After the initial MRI tumor-bearing mice were then treated for 6 constitutive days with 10 mg/Kg DEX or vehicle (solvent for DEX). After the completion of treatment mice were followed for neurological signs of tumor burden that were used to determine the survival endpoint in humane fashion and accordance with IACUC protocols. Right before sacrificing each symptomatic tumor-bearing mouse was re-imaged again in order to determine the volume that caused the neurological signs. Similar to the results observed with B20, DEX treated mice lived longer with larger tumors compared to controls. The new data are now included as (**Fig. 6A,-D**).*

To examine potential effects of DEX on angiogenesis, we examined the effect DEX treatment had on total vessel area or average vessels size. In contrast to B20 treatment, we did not see significant changes in either total vessel area or average vessel size in the DEX treated animals. The new data are now incorporated in ***Figure 6E-F.***

COMMENT: A study cited in the present manuscript (J Clin Oncol. 2015 Sep 1;33(25):2735-44) showed that concomitant radio-chemotherapy and anti-angiogenesis (with the VEGF-A blocker bevacizumab) prolonged overall survival in patients with proneural GBM. This effect cannot be seen in the (proneural) glioma mouse model. Is there an explanation for the differences between preclinical models and clinical data?

RESPONSE: *The Sandmann paper is very interesting, but hypothesis-generating at best. It requires independent confirmation. Moreover, this finding is a group effect and by no means predicts that all proneural-like glioblastomas would benefit from Bevacizumab. Besides, the primary goal of our murine studies was not to determine anti-tumor or the effects of B20-4.1.1 when combined with RT on survival of the tumor-bearing mice. Our primary goal was to determine whether we can achieve the anti-edema effect of B20-4.1.1 using low dose and short treatment paradigm. Understanding how blocking VGEFA in PN hGBM enhances RT efficacy is beyond the scope of this manuscript and will require different primary goals and set of experiments and different doses of B20-4.1.1 and longer time of treatment that may be needed to achieve maximum anti-cancer efficacy alone or in combination with RT.*

COMMENT: The benefits of bevacizumab on progression-free survival are discussed. However, it is not mentioned that the inability to detect glioma progression after bevacizumab treatment likely is attributed to imaging artifacts and does not reflect therapeutic effects in front-line treatment (BMC Cancer. 2009 Dec 16;9:444).

RESPONSE: *This has been discussed and the reference by Verhoeff et. al., in BMC Cancer. 2009 Dec 16;9:444 is now included in the manuscript. Additionally, in the edema analysis of our mouse model (Figure 6A-D), the B20-4.1.1 tumor volumes are quantified using both T1-post*

contrast and T2 weight MRI, which has been clarified in the manuscript. our mouse model we have clarified

COMMENT: Figure 1A: According to the results part, Figure 1A compared the overall survival between patients not on DEX and patients on DEX. However, it was not clear what red curve and black curve in the Fig.1A represented.

***RESPONSE**: We apologize – this information has been added.*

COMMENT: Figure 1C: According to the result part in page 6, Fig. 1c showed that OS was inferior in the steroid-exposed patients. However, the p value of the log-rank test was reported neither in the text nor in the figure 1c.

***RESPONSE**: Figure 1C has a p value now.*

COMMENT: Also, there were 1029 GBM patients in the GNN cohort. However, in the figrue1c, N=462 with No-steroids group, and N=370 with steroids group. The total sample size of these two groups (N=832) did not equal to the cohort sample size (N=1029).

***RESPONSE:** We have now restricted the analysis primarily to patients where the data were available for multivariate analysis. We hope this makes it clearer.*

COMMENT: Table S1B: In Table S1A, the result revealed that KPS, Mental status, neurologic functional status, surgical extent, radiation dose, RPA class were statistically significant between the two groups (N=522 vs. N=100). Thus, these factors should be considered in the multivariate analysis in Table S1B. However, only RPA class was adjusted.

***RESPONSE**: We apologize for the confusion. The RPA classification is a composite that takes into account the various clinical prognostic features (age, KPS, mental status, neurological functioning, extent of surgery, and total radiation dose). When we reanalyze the MSKCC dataset with either a continuous or categorical multivariate analysis taking these variables into account individually, we find that steroid use remains statistically significantly and independently associated with survival. For simplicity, we did not present that information in the manuscript, but are happy to include it here and can incorporate it into the supplemental data if desired.*

Categorical Multivariate Analysis

Variables	*p*Values	HR	95% CI
Age (≥50)	$p < 0.0001$ ***	1.535	1.2573 - 1.8748
KPS (<70)	**$p = 0.0719$ (ns)**	**1.318**	**0.9757 - 1.7811**
Resection vs Biopsy	$p < 0.0001$ ***	0.631	0.5041 - 0.7907
RT Dose >54.4Gy	**$p < 0.0001$ *** **	**2.120**	**1.6562 - 2.7140**
Symptons <12 weeks	$p = 0.5793$ (ns)	1.066	0.8505 - 1.3359
Neuro Function	**$p < 0.0001$ *** **	**0.689**	**0.5709 - 0.8318**
MMSE	$p = 0.6256$ (ns)	0.945	0.7534 - 1.1856
Temozolomide	**$p < 0.0001$ *** **	**0.740**	**0.6190 - 0.8852**
DEX	$p = 0.0053$ **	1.397	1.1044 - 1.7677

Continuous Multivariate Analysis

Variables	*p*Values	HR	95% CI
Age	$p < 0.0001$ ***	1.023	1.0162 - 1.0307
KPS	**$p = 0.0719$ (ns)**	**0.998**	**0.9896 - 1.0062**
GTR vs Biopsy	$p < 0.0001$ ***	0.481	0.3743 - 0.6176
STR vs Biopsy	**$p = 0.0059$ ****	**0.720**	**0.5694 - 0.9096**
RT Dose (Gy)	$p < 0.0001$ ***	0.9682	0.9585 - 0.9779
Symptons (weeks)	**$p < 0.0001$ *** **	**1.001**	**0.9986 - 1.0029**
Neuro Function	$p = 0.0082$ **	0.769	0.6328 - 0.9344
MMSE	**$p = 0.7440$**	**1.039**	**0.8275 - 1.3034**
Temozolomide	$p < 0.0001$ ***	0.706	0.5913 - 0.8434
DEX	**$p = 0.01173$ ***	**1.359**	**1.0706 - 1.7256**

COMMENT: Results (Page 5, last sentence): "After adjustment, this effect remained significant (p=0.03)." It was not clear what factors was adjusted here.

RESPONSE: *For all survival analyses, adjustment factors were: Extent of surgery, age, WHO performance status. This was added at the first occurrence, removed later.*

COMMENT: Retrospective clinical analyzes (Page 35, the fourth paragraph): Description of the statistical method was not found in the MSKCC cohort.

RESPONSE*: We apologize for the lack of clarity, and have updated the supplemental materials to better describe the process.*

"Categorical multivariate cox regression models were constructed correlating RTOG class, initial chemotherapy use, and baseline corticosteroid use with clinical outcomes."

COMMENT: Besides, patients and treatment characteristics between the groups were analyzed in MSKCC cohort but was not found in EORTC trial and GNN cohort.

RESPONSE: *New tables for both EORTC and GGN trial are now included as new Supplemental Table 2A,B, correspondingly..*

COMMENT: Results (Page 7, the last sentence in the second paragraph): P value was not reported here.

RESPONSE: *We apologize – P value has been added*

COMMENT: Figure 5B: In the figure legend of figure 5 (page14), it was not clear what was "paired ANOVA analysis".

RESPONSE: *Paired ANOVA analysis was used for analysis of results in Figure 5B. The study was designed to use BLI as readout of the effects of DEX on tumor proliferation at 0, 24 and 48h post DEX and vehicle treatments. In this study each mouse with a tumor was measured by BLI at start of the treatment (0 point), 24h and 48h post treatment. There is more than one repeated factor present in these measures (three time imaging the same mouse). In cases with the same samples measured a multiple times standard ANOVA can't be used and paired ANOVA is recommended.*

COMMENT: Figure 6G: P value of the survival analysis was reported neither in the figure nor the figure legend.

RESPONSE*: We apologize –P values and median survival times have now been added.*

COMMENT: Previous phase II clinical trial has demonstrated dosing effect of DEX when combing with TTfield therapy (Wong ET et al. 2014 Cancer Med). Are there any difference in the high and the low dose of DEX on patient survival?

***RESPONSE**: The Wong et al. 2015 study raises an interesting question as to how the immunosuppressive effects of DEX might interfere with ongoing therapy. In addition to immunosuppression from DEX, RT and temozolomide are in their own right immunosuppressive, and it remains to be determined how strongly DEX influences the immune response as a single agent. Unfortunately, in our retrospective datasets we don't have access to total cumulative dose of steroids used. However we do have some dose information for the EORTC dataset, which we have included in the manuscript. When stratified by tercile in univariate analysis, the steroid dose is significantly pognositc in progression free and overall survival (PFS p=0.03, HR=1.14, OS p=0.002, HR=1.2) . However, it is not significant when performing multivariate analysis (PFS p=0.45, OS p=0.23)* We have also updated our manuscript to include discussion of the *Wong et. al., reference (Wong et al., 2015).*

COMMENT: There are no clear molecular mechanisms proposed by the authors regarding the how DEX reduce the therapeutic efficacy of the anit-glioma radiation therapy. Authors proposed that based on another study p21 expression associated with radioresistance phenomena in GBM. But they did not provide any data regarding the p21 status. They demonstrated that DEX therapy significantly reduced the tumor burden represented by the BLI signal (Fig. 5 A&B) but the endpoint survival data show DEX treatment don't have any effect (Fig 4 A). In light of these data it is safe to conclude that BLI data is not correct, and author should consider removing it.

***RESPONSE:** The decrease seen with the BLI signal using E2F1-luc mouse does not represent decrease in tumor burden. It demonstrates a decrease in proliferation, which is in agreement with the staining for PCNA as well as Ki67, which now is included in the manuscript as Supplemental Figure 1A. Considering the treatment paradigm (only 3 days), the amount decrease of proliferation and lack of effect on cell death it is not surprising that DEX has no effect on survival of tumor-bearing mice.*

Previously we have tried a number of p21 antibodies to inquire if the cells high p21 are radioresistant. Unfortunately, p21 antiboides were unsuccessful in our model and we were unable to produce consistent staining that would allow us to draw conclusions.

COMMENT: Even though the authors have shown that the proliferation is decreased upon DEX therapy represented by the percent of PCNA positive cells (Fig. 5D), the biological significant percent of PCNA cells decreasing about 15-20% and its role in altering the therapeutic efficacy of the radiotherapy was not explored. How about the DNA repair capacity during DEX therapy? It has been shown that DEX can alter the DNA repair gene such as MGMT (Grombacher et al. 1996 Carcinogenesis). Authors need to explore the possible molecular mechanism.

***RESPONSE:** This is an interesting comment based on studies using rodent hepatoma cells, but the proposed effect may not hold true for glioma cells: our previous studies indicated that dexamethasone at clinically achieved concentrations of up to 100 nM for 28 h did not modulate MGMT activity in any of the 12 human glioma cell lines and dexamethasone at 100 nM did not*

modulate the effects of TMZ in T98G and LNT-229 cells in acute growth inhibition or clonogenic cell death assays (Hermisson et al., 2006). 15-20% decrease in total PCNA when translated into olig2/PCNA double positive, which are the tumor cells, results in 30% decrease in glioma cell proliferation, which is close what we also see by BLI.

COMMENT: Authors reported 18 genes gene signature in glioma in response to DEX. What are these genes? They should discuss these genes and their pathway in their discussion.
We apologize for the oversight, supplementary table describing the genes involved and ingenuity pathway analysis of these genes is now included (Supplementary Table S4). Pathway analysis shows that the DEX gene signature is enriched for genes involved in cell cycle signaling, mitotic assembly, and DNA repair check points. This is now highlighted in the discussion.

COMMENT: The manuscript requires careful revision. There are many careless mistakes. For example Fig. 7 and fig.8 are completely switched. Some of the statistics is questionable and require further analysis (For example Fig. 6D right graph she statistically significant even though the error bar seems to be overlapping).

RESPONSE: *We apologize for mistakes and now carefully revised the manuscript.*

References:

Ellsworth S, Grossman SA. Comment on 'Dexamethasone exerts profound immunologic interference on treatment efficacy for recurrent glioblastoma'. Br J Cancer 2015; 113(11): 1632-3.

Feng X, Szulzewsky F, Yerevanian A, Chen Z, Heinzmann D, Rasmussen RD*, et al.* Loss of CX3CR1 increases accumulation of inflammatory monocytes and promotes gliomagenesis. Oncotarget 2015; 6(17): 15077-94.

Hambardzumyan D, Gutmann DH, Kettenmann H. The role of microglia and macrophages in glioma maintenance and progression. Nat Neurosci 2015; 19(1): 20-7.

Hermisson M, Klumpp A, Wick W, Wischhusen J, Nagel G, Roos W*, et al.* O6-methylguanine DNA methyltransferase and p53 status predict temozolomide sensitivity in human malignant glioma cells. J Neurochem 2006; 96(3): 766-76.

Lu-Emerson C, Snuderl M, Kirkpatrick ND, Goveia J, Davidson C, Huang Y*, et al.* Increase in tumor-associated macrophages after antiangiogenic therapy is associated with poor survival among patients with recurrent glioblastoma. Neuro Oncol 2013; 15(8): 1079-87.

Wong ET, Lok E, Gautam S, Swanson KD. Dexamethasone exerts profound immunologic interference on treatment efficacy for recurrent glioblastoma. Br J Cancer 2015; 113(11): 1642.

CORTICOSTEROIDS COMPROMISE SURVIVAL IN GLIOBLASTOMA

Kenneth L. Pitter[1*], Ilaria Tamagno[2*], Kristina Alikhanyan[3], Amira Hosni-Ahmed[4¶], Siobhan S. Pattwell[5], Shannon Donnola[2§], Charles Dai[2], Tatsuya Ozawa[5], Maria Chang[6], Timothy A. Chan[6,7], Kathryn Beal[6,7], Andrew J. Bishop[6], Christopher A. Barker[6], Terreia S. Jones[4], Bettina Hentschel[8], Thierry Gorlia[9], Uwe Schlegel[10], Roger Stupp[11], Michael Weller[12#], Eric C. Holland[5,13,14#], Dolores Hambardzumyan[2,3#].

[1]Department of Cancer Biology and Genetics, Memorial Sloan-Kettering Cancer Center, New York, NY 10065, USA. [2]Department of Neurosciences at the Cleveland Clinic Lerner Research Institute, Cleveland, Ohio, 44195, USA. [3]Department of Pediatrics, Aflac Cancer and Blood Disorders Center, Children's Healthcare of Atlanta, Emory University School of Medicine, Atlanta, GA, USA. [4]University of Tennessee Health Science Center, Department of Clinical Pharmacy, Memphis, TN, 39103, USA. [5]Division of Human Biology, Fred Hutchinson Cancer Research Center, Seattle, WA 98109, USA (FH). [6]Department of Radiation Oncology, Memorial Sloan-Kettering Cancer Center, New York, NY 10065, USA. [7] Human Oncology and Pathogenesis Program, Memorial Sloan-Kettering Cancer Center, New York, NY 10065, USA. [8]Institute for Medical Informatics, Statistics and Epidemiology, University of Leipzig, Leipzig, Gemany. [9]European Organisation for Research and Treatment of Cancer, Brussels, Belgium. [10]Department of Neurology, University Hospital Knappschaftskrankenhaus Bochum-Langendreer, Bochum, Germany. Departments of [11]Oncology and [12]Neurology, University Hospital and University of Zurich, CH-8091 Zurich, Switzerland. [13]Alvord Brain Tumor Center and Department of Neurosurgery, University of Washington, Seattle, WA 98109, USA (UW), [14] Solid Tumor and Translational Research (FH) and (UW) and [3]Department of Pediatrics, Aflac Cancer and Blood Disorders Center, Children's Healthcare of Atlanta, Emory University School of Medicine, Atlanta, GA, USA.

[*, #] Authors contributed equally.

Corresponding Authors: Current address is

DH: 1760 Haygood Drive, E-380, Atlanta, 30329, GA, USA. Tel: 404727-3720. Fax: 404-727-4455. Email- dhambar@emory.edu

ECH: 1100 Fairview Avenue N., Seattle, WA 98109, USA. Tel: (206) 667-6117. Fax: (206) 667-7850 USA. Email: eholland@fhcrc.org.

MW: Frauenklinikstrasse 26, CH-8091, Zürich, Switzerland. Tel: 41 44 255 5500. Fax: 41 44 255 4507. E-mail: michael.weller@usz.ch

§ Current address: Department of Radiology at Case Western Reserve University, Cleveland, OH

[¶] Current address: Department of Chemistry, College of Science, Fayoum University, Fayoum, Egypt.

Running Title: Corticosteroids compromise survival in glioblastoma

ABSTRACT

Glioblastoma is the most common and most aggressive primary brain tumor (Ostrom *et al.*, 2014). Standard of care consists of surgical resection followed by radiotherapy and concomitant and maintenance temozolomide (TMZ/RT→TMZ). Corticosteroids are commonly used perioperatively to control cerebral edema and are frequently continued throughout subsequent treatment, notably RT, for amelioration of side effects. The effects of corticosteroids such as dexamethasone (DEX) on cell growth in glioma models and on patient survival have remained controversial.

We performed a retrospective analysis of glioblastoma patient cohorts to determine the prognostic role of steroid administration. A disease-relevant mouse model of glioblastoma was used to characterize the effects of DEX on tumor cell proliferation and death, and to identify gene signatures associated with these effects. A murine anti-VEGFA antibody was used in parallel as an alternative for edema control. We applied the DEX-induced gene signature to the TCGA glioblastoma dataset to explore the association of DEX exposure with outcome. Mouse experiments were used to validate the effects of DEX on survival *in vivo*.

Retrospective clinical analyses identified corticosteroid use during RT as an independent indicator of shorter survival in three independent patient cohorts. A DEX-associated gene expression signature correlated with shorter survival in the TCGA patient dataset. In glioma-bearing mice, DEX pretreatment decreased tumor cell proliferation without

affecting tumor cell viability, but reduced survival when combined with RT. Conversely, anti-VEGFA antibody decreased proliferation and increased tumor cell death, but did not affect survival when combined with RT.

Clinical and mouse experimental data suggest that corticosteroids may decrease the effectiveness of treatment and shorten survival in glioblastoma. DEX-induced anti-proliferative effects may confer protection from RT-and chemotherapy-induced genotoxic stress. This study highlights the importance of identifying alternative agents such as VEGF antagonists for managing edema in glioblastoma patients. Beyond the established adverse effect profile of protracted corticosteroid use, this analysis substantiates the request for prudent and restricted use of corticosteroids in glioblastoma.

INTRODUCTION

Dexamethasone (DEX) is a potent synthetic corticosteroid and is considered the "gold standard" for managing cerebral edema (Raslan and Bhardwaj, 2007). The exact mechanism underlying the anti-edema effects of DEX is not known, although it is widely believed that DEX suppresses inflammation and decreases vasogenic edema through partial restoration of blood-brain barrier integrity (Rovit and Hagan, 1968; Eisenberg *et al.*, 1970; Kotsarini *et al.*, 2010). It is also not clear whether DEX influences the effectiveness of standard DNA-damaging therapy for glioblastoma such as radiotherapy (RT) or alkylating agents. There are conflicting studies *in vitro* (Grasso *et al.*, 1977; Weller *et al.*, 1997) and *in vivo* (Wang *et al.*, 2004) that show antagonism, no interaction, or even synergy with chemotherapy (reviewed in Piette *et al.*, 2006). Despite uncertainty regarding biological efficacy in glioblastoma, DEX is effective in controlling many RT- and chemotherapy-induced side effects (i.e. nausea and vomiting) and is therefore frequently continued throughout the duration of RT. More recently, it has been observed that VEGF antagonists such as the antibody, bevacizumab, or the tyrosine kinase

inhibitor, cediranib, have profound anti-edema effects, commonly obviating the need for steroid comedication if administered to patients.

In the present study, we confirmed the use of corticosteroids early in the course of disease, during RT without or with chemotherapy, as an independent predictor of poor outcome in three independent patient cohorts. We also used disease-relevant genetically engineered mouse models (GEMMs) of murine glioblastoma (Hambardzumyan *et al.*, 2009) to show that DEX pretreatment significantly decreases survival in irradiated glioma-bearing mice. Finally, we report that replacing DEX with short-term VEGF antagonism may be the preferred alternative over corticosteroids in the initial management of glioblastoma.

Methods

Retrospective Clinical Analyses

Three independent patients cohort were analyzed. Details are provided in the Supplementary Appendix.

Generation of RCAS/Tva system-based PDGFB-driven and orthotopic gliomas

6-8-week-old *Ntv-a/ink4a-arf-/-, Gli-luc;Ntv-a;Ink4a-Arf*$^{-/-}$ and *N-tva/*Ef-Luc mice were used to generate gliomas via introduction of RCAS-PDGFB-HA and RACS-shp53 (Uhrbom *et al.*, 2004; Hambardzumyan *et al.*, 2009). Details are provided in the Supplementary Appendix.

MRI scans

T2-weighted and T1-weighted contrast-enhanced MRI scans of tumor-bearing mice were performed as described (Koutcher *et al.*, 2002).

Tissue Processing, Immunohistochemistry and Immunofluorescence

These assays were performed according to previously published protocols (Becher *et al.*, 2008; Hambardzumyan *et al.*, 2008) and antibody information is provided in the Supplementary Appendix.

Bioluminescence imaging (BLI)

Ef-Luc mice were used for BLI studies according to published protocols (Uhrbom *et al.*, 2004). Additional methodological details are provided in the Supplementary Appendix.

RESULTS

Retrospective clinical analyses of glioblastoma patients

To investigate an association of corticosteroid use with the efficacy of therapy and outcome, we first performed a retrospective clinical analysis of 622 patients treated at Memorial Sloan Kettering Cancer Center (MSKCC). Expectedly (Stupp *et al.*, 2005), patients receiving TMZ had a significantly longer median survival (15.9 vs. 12.8; p=0.0023). Patients not on DEX at the start of RT had a median survival of 20.6 months whereas patients on DEX had a survival time of 12.9 months (p<0.0001, **Fig. 1A**). There were no significant differences in age, gender, duration of symptoms, or TMZ use between patients that did or did not receive steroids at the start of therapy. Steroid use was significantly more common in patients with lower KPS, altered mental status, altered neurologic function, less extensive surgery, and lower radiation dosing. Accordingly, steroid use was significantly more common in the higher RPA groups (**Table S1A**). Yet, multivariate COX regression analysis revealed that OS was independently associated with RPA class, TMZ use and steroid use at the start of RT (**Table S1B**).

Second, we also explored the association of baseline steroid use with outcome in 573 patients from the pivotal EORTC NCIC trial that established TMZ/RT→TMZ as the new standard of care (Gorlia *et al.*, 2008; Stupp *et al.*, 2014). The use of steroids was correlated with the extent of resection at initial surgery (p<0.0001, Fisher test); 91% of patients who underwent biopsy, 74% of patients with partial resection, but only 59% of

patients with complete resection had steroids at baseline (**Table S2A**). The median dose administered was 12 mg for biopsied patients and 6 mg for patients with partial or complete resection ($p>0.0001$, Kruskal-Wallis test). Patients with baseline steroids had a lower median PFS (5.3 vs. 6.4, $p<0.0001$, HR=1.39). After adjustment for the extent of surgery (partial or complete resection vs biopsy), age (continuous), WHO performance status (>0 vs 0), this effect remained significant ($p=0.03$) stratified by treatment (**Table S3A**). This effect was borderline, non-significant in the RT arm ($p=0.06$, HR=1.33) whereas it was not significant in the TMZ/RT→TMZ arm ($p=0.23$, HR=1.17). The prognostic value of baseline steroid dose (split by tercile) was significantly overall stratified by treatment ($p=0.03$, HR=1.14) but not in multivariate analysis ($p=0.45$). Steroid dose was significant in the RT arm ($p=0.004$, HR=1.28) but was borderline, non-significant in multivariate analysis ($p=0.08$) and was not significant in the TMZ/RT→TMZ arm ($p=0.8$, HR=1.02; $p=0.88$ in multivariate analysis). Altogether, patients with baseline steroids had a lower median OS (12 vs. 17 months, $p<0.0001$, HR=1.56) (**Fig. 1B**). This effect remained significant after adjustment for age, extent of surgery, and WHO performance status ($p=0.003$) and was significant in the RT arm ($p=0.004$, HR=1.52) but not in the TMZ/RT→TMZ arm ($p=0.2$, HR=1.2). The prognostic value of steroid dose at baseline, split by tercile, was significantly when stratified by treatment ($p = 0.002$, HR=1.2) but not significant in multivariate analysis ($p = 0.23$). Steroid dose was significant in the RT arm ($p=0.002$, HR=1.28) and in multivariate analysis ($p=0.048$). It was not significant in the TMZ/RT→TMZ arm ($p=0.22$, HR=1.11, also not significant in the multivariate model, $p=0.73$). Thus, steroids at baseline was a prognostic factor for both PFS and OS in the EORTC NCIC trial and higher doses of steroids were a negative prognostic factor in patients treated with RT alone more than in patients treated with TMZ/RT→TMZ.

Third, an association between steroid administration at the start of RT and outcome was examined in a cohort of 832 glioblastoma patients enrolled in the German Glioma Network (GGN) (**Table S2B**). PFS and OS were inferior in steroid-exposed patients in all patients pooled (**Fig. 1C**, **Fig. 2A, Table S3B**) as well as in patients treated with RT plus chemotherapy, although not patients treated initially with RT alone (**Fig. 2B-D, Table**

S3B). The association between steroids and inferior outcome was prominent in patients who had received a gross total resection, notably in those treated with RT plus chemotherapy (**Fig. 3**; **Table S3B**). Multivariate analysis confirmed that steroid administration was an independent negative prognostic factor when adjusting for extent of resection, initial treatment, age and KPS (**Table S3B**).

DEX, but not anti-VEGFA antibodies, compromise RT efficacy in murine glioma models *in vivo*.

In order to support potential adverse effects of DEX on survival, we utilized a murine PDGFB-driven glioblastoma model, based on the RCAS/Tva system, a somatic cell specific gene transfer (Hambardzumyan *et al.*, 2009). DEX alone had no impact on survival (p=0.32, **Fig. 4A**) whereas pretreatment with single doses of DEX for three constitutive days profoundly decreased the survival advantage afforded by a single 10 Gy dose of irradiation (p=0.03, **Fig. 4B**). This effect was even more pronounced when a fractionated irradiation schedule was used (p=0.002, **Fig. 4C**).

Because of the deleterious effects of DEX on the survival benefit afforded by RT, we next focused on identifying an alternative to DEX to decrease edema. Inhibition of VEGF signaling, either with neutralizing antibodies or VEGFR-targeted kinase inhibitors, leads to decreased edema, which can result in improved survival of brain tumor-bearing mice despite persistent tumor growth (Gerstner *et al.*, 2009; Kamoun *et al.*, 2009). In order to assess whether the anti-VEGF antibody-B20-4.1.1, a murine surrogate for bevacizumab, interferes with the response to RT, too, we allocated tumor-bearing mice into different treatment groups based on gender and age. Compared to vehicle treatment, both B20-4.1.1 and RT independently prolonged survival (**Fig. 4D**). However, in contrast to DEX, there was no significant difference between B20-4.1.1+RT treated animals compared to RT alone, demonstrating that B20-4.1.1 treatment does not interfere with RT efficacy (p=0.86, **Fig. 4D**).

DEX responsive gene signature in gliomas.

In order to broadly assess the genes and pathways that are responsive to DEX and identify pathways associated with treatment resistance, we utilized microarray analyses from untreated and DEX-treated mouse glioma samples. The data were first analyzed by principle component analyses (PCA) (**Fig. 5A**). We identified nineteen genes that were significantly altered (all down-regulated) in response to DEX treatment, seven of which were subsequently validated by quantitative real-time PCR **(Fig. 5B,C)**. These genes were significant components of the cell cycle and mitotic machinery **(Table S4).**

We generated a DEX-responsive signature based on the arrays described above and queried TCGA patient survival and expression data. Because DEX is given to essentially all patients prior to surgery, we predicted that they would have expression signatures reflecting DEX treatment. We further identified a subset of patients with a comparatively high expression of genes down-regulated by DEX as having tumors that are minimally responsive to DEX treatment (**Fig. 5D**). High expression was defined as greater than two standard deviations above the mean, which classified 13% of patients as minimally responsive ("Untreated-Like"; **Fig. 5E**). These patients had the highest expression levels of one or more of the DEX down-regulated genes and had a significantly longer median survival (p=0.008, **Fig. 5F**). Our TCGA analysis was suggestive of an improved survival for patients whose tumors reflected our untreated mouse samples compared to DEX-treated samples.

DEX treatment effects on glioma growth *in vivo* and *in vitro*

One mechanistic explanation of drugs compromising RT efficacy is based on the phenomenon that, in general, cells are more radiosensitive when they are in G2/M and more radioresistant when they are in G1. Therefore if a drug induces a decrease in proliferation, it can potentially reduce the radiosensitivity of a population via redistribution of the cell cycle, leading to accumulation in G1 and decreased fractions in G2/M (Powell and Abraham, 1994). We have previously documented that DEX induces the cell cycle inhibitor p21 (Glaser *et al.*, 2001), and overexpression of p21 is associated

with radioresistance in human gliomas (Kokunai and Tamaki, 1999). Accordingly, we next examined DEX effects on proliferation of tumor cells *in vivo*. We first set out to assess the effect of DEX on proliferation of mouse gliomas using a non-invasive bioluminescence (BLI) reporter. We have previously described a *Ntv-a;*Ef-Luc transgenic mouse that expresses firefly luciferase driven by the *E2F1* promoter (Ef-Luc) (Uhrbom *et al.*, 2004). The E2F1 transcription factor is normally activated in cell cycle progression during the G1/S transition and is highly active in gliomas (Parr *et al.*, 1997). The dose of DEX used in the clinic for patients with high grade gliomas is variable, ranging from 0.5 to 16 mg daily (discussed in detail in (Kostaras *et al.*, 2014)). Considering the toxicity associated with higher doses of DEX and the wide range of doses used in human patients, we used doses closer to the lower end of the range, 0.81 mg daily, which based on dose translation from human studies equals approximately 10 mg/kg (Reagan-Shaw *et al.*, 2008). First, we confirmed that 10 mg/kg DEX was not toxic in non-tumor-bearing mice when given at that dose for seven days and followed for 45 days (data not shown). Next, tumor-bearing mice were imaged by BLI and then randomized into either vehicle or DEX-treated cohorts (daily DEX i.p. at 10 mg/kg) and followed for 48 h **(Fig. 6A)**. Vehicle-treated mice showed no change in BLI signal ($p=0.35$, **Fig. 6B**) while there was a decrease in BLI with DEX treatment ($p=0.0006$, **Fig. 6B)**. In our model, glioma cells express high levels of Olig2, which can be used to distinguish the bulk tumor from stromal cells (Helmy *et al.*, 2012). To specifically address the anti-proliferative effect of DEX on tumor cells, we utilized immunofluorescence double staining for Olig2 and PCNA (**Fig. 6C**) and showed a specific decrease in tumor cell proliferation in DEX-treated mice ($p<0.0001$, **Fig. 6D**), which was also confirmed with Ki67 staining, a second marker of proliferation (**SFig. 1A**). Comparing areas of necrosis and levels of the pro-apoptotic cleaved caspase-3 revealed no significant differences between groups, confirming that the decrease in proliferation was due to a cytostatic effect and not due to overall cell loss (**Fig. S1B**).

In order to further characterize the effects of DEX on proliferation *in vitro*, we generated mouse primary glioma cell cultures. When different doses of DEX were tested in brain tumor patients, the average concentration of DEX in tumor tissue was approximately 225 ng/g (about 225.27 ng/ml) (Nestler *et al.*, 2002). We chose three concentrations of DEX

(39.5 ng/ml=0.1 μM, 395 ng/ml=1 μM and 3950 ng/ml=10 μM). In contrast to the results of tumors *in vivo*, none of the murine cell lines tested showed a significant decrease in growth or viability (**Fig. S2A**). Next, we compared the cell cycle profile of primary cultures treated with or without DEX **(Fig. S2B)**. There was a marginal increase in G1 and a marginal decrease in G2, which may explain why we did not observe a difference in growth or viability. Taken together, these assays suggest that the *in vivo* effects of DEX are not recapitulated *in vitro*, highlighting the importance of using an *in vivo* system with an intact tumor microenvironment. These data imply that the *in vivo* effect of DEX on tumor cell proliferation is probably indirect.

Effects of DEX and anti-VEGFA antibody on edema and in vivo glioma growth

It has been well-documented that inhibition of VEGF signaling, either with neutralizing antibodies or VEGFR-targeted kinase inhibitors decreases edema, resulting in improved survival of brain tumor-bearing mice despite persistent tumor growth (Gerstner *et al.*, 2009; Kamoun *et al.*, 2009). Therefore, we examined the tumor size at onset of neurological symptoms, such as seizure, lethargy, or weight loss, of vehicle, DEX, and B20-4.1.1 treated animals, reasoning that effective edema treatment would permit larger tumors at the time of onset of symptoms. Based on MRI-determined tumor volume, asymptomatic glioma-bearing mice were randomized into vehicle, DEX or B20-4.1.1 treatment groups. Animals were treated with their respective agent and subsequently reimaged upon time of symptom development. Although DEX treatment alone offered no survival advantage, DEX treated animals had significantly larger tumors at the time of symptom onset (**Fig 6B**). Despite controlling edema and permitting mice to remain asymptomatic with larger tumors, there was no survival advantage to DEX treatment alone (**Fig 6A**). Interestingly, in B20-4.1.1 treated animals we saw a significant survival advantage as well as significantly larger tumors at the end point of survival than vehicle-treated mice (**Fig. 6C,D)**. This was also true when quantified by T1-contrast enhancement **(SFig. 3B**).

The effects of DEX and Anti-VEGFA antibody on tumor vasculature and associated myeloid cells infiltration.

As both DEX and B20-4.1.1 were effective in controlling edema, we next investigated their effects on tumor vasculature by immunohistochemistry. Sections of mouse gliomas treated with vehicles and either B20-4.1.1 or DEX were stained with anti-CD31 antibody, which specifically labels endothelial cells of glioblastoma and normal blood vessels outside of the tumor area. In DEX-treated tumors we saw no changes either in total vessel area or average vessel size compared to vehicle (**Fig. 6E,F**). B20-4.1.1 tumors had decreases in total vessel area ($p < 0.0001$) and average vessel size ($p=0.0076$), while no differences were observed in non-tumor cortical areas (**Fig. 6G,H, SFig. 3A**). Decrease in total vessel area and average vessel size induced by B20-4.1.1 was transient since vessels returned to their initial morphology when B20-4.1.1 was stopped (data not shown). We further investigated the effect of B20-4.1.1 on tumor vasculature using Hoechst dye leakage assays and functional vessel labeling with circulating FITC-conjugated lectin in vehicle- and B20-4.1.1-treated tumors (**Fig. 6I,J**). B20-4.1.1 decreased leaky areas compared to vehicle (**Fig. 6E,F**) ($p=0.002$).

DEX was suggested to be immunosuppressant, as are RT and TMZ (Ellsworth and Grossman, 2015), and a **r**ecent correlative study suggested that DEX-treatment induced immune suppression could interfere with clinical efficacy of standard therapy in recurrent glioblastoma (Wong *et al.*, 2015). Microglia/macrophages are the major immune infiltrates in both murine and human glioblastoma, accounting for up to 20-30 % of the total tumor mass (Feng *et al.*, 2015; Hambardzumyan *et al.*, 2015).

To investigate potential immunosuppressive characteristics of DEX we looked at the numbers of infiltrated tumor-associated microglia/macrophages in response to either DEX or VEGFA antibody treatment using the myeloid lineage marker Iba1. No difference was observed between DEX-treated and vehicle treated tumors (**SFig. 3C upper panel**), whereas we observed a significant increase in Iba1 positive microglia/macrophage infiltration in B20-4.1.1 treated mice when compared to vehicle (**SFig. 3C lower panel**),

Anti-VEGFA antibody B20-4.1.1 decreases glioma proliferation and induces tumor cell death.

In our mouse model, DEX treatment alone offers no survival advantage whereas B20-4.1.1 alone consistently prolonged survival (**Fig. 4A,D; Fig. 6**). To examine potential effects on proliferation, we treated tumor-bearing mice with vehicle or B20-4.1.1 for two weeks (5 mg/kg B20-4.1.1 twice a week) and compared the proliferation of tumor cells by double staining for Olig2 and PCNA. We observed a significant decrease in proliferation of tumor cells in B20-4.1.1-treated samples ($p < 0.0001$, **Fig. 7A,B**). Similarly, we confirmed this reduction in both Ki67 staining and in pH3 staining (**data not shown**).

Next, we examined whether B20-4.1.1 promotes cell death in gliomas. B20-4.1.1 treated tumors had a decrease in the Olig2-positive tumor area ($p=0.02$, **Fig. 7C,E**) and an increase in apoptotic cells, as evidence by increased TUNEL-positivity ($p=0.02$, **Fig. 7D,F**). To address whether it is only tumor cells or other non-neoplastic cells in the tumor microenvironment that are affected by B20-4.1.1 treatment, we performed immunofluorescence double staining for TUNEL and the tumor-specific marker Olig2, the endothelial cell-specific marker CD31, the microglia/macrophage-specific marker Iba1, or the reactive astrocyte-specific marker GFAP. In vehicle-treated tumors, 1.01% of TUNEL-positive cells were also Olig2-positive, which was significantly increased to 3.55% in B20-4.1.1-treated mice ($p=0.03$) (**Fig. S4A,B**). We did not observe significant changes in the number of TUNEL-positive cells from the tumor microenvironment (**Fig. S4A,B;** data now shown)

DISCUSSION

The administration of steroids to control neurological morbidity associated with brain tumors has been established as a standard of care decades ago. Except for primary CNS lymphoma where steroids exert direct cytotoxic effects, amelioration of brain tumor-association edema has been proposed to underlie these symptomatic effects of steroids.

However, these undisputed beneficial effects of steroids have to be weighed against a plethora of acute and long-term side effects.

In the current study, we identified the use of corticosteroids early in the disease course, during RT without or with alkylating chemotherapy, as an independent predictor of poor outcome in three independent patient cohorts. Although higher steroid doses are commonly given to patients with larger tumors and more prominent neurological deficits, we tried to control for such unfavorable confounders as feasible. Yet, we cannot exclude that detrimental effects of steroids other than direct interference with RT contributed to the overall inferior outcome of patients exposed to steroids. Thus, steroids can contribute to morbidity and mortality through their direct toxicity, including steroid myopathy, impaired immune function, adrenal insufficiency, and bowel perforation. Our findings with three large independent dataset were further supported with a recent correlative retrospective analysis of 73 patients with glioblastoma showing that DEX use during RT with concurrent TMZ correlated with reduced OS and PFS (Shields *et al.*, 2015).

In support of a direct detrimental effect interfering with the activity of RT, we report that pretreatment with DEX decreased the survival benefit afforded by RT in murine gliomas. In these tumors, DEX decreased proliferation and the expression of many cell cycle-related genes. Expression of these genes inversely correlated with survival in the TCGA glioblastoma patient dataset. Of note, these genes are primarily known or predicted to be involved in proliferation, either via cell mitotic assembly, cycle checkpoints, DNA damage response and ATM signaling. RT sensitivity varies with the position of the cells in the cell cycle, and in general, tumors with high cell turnover rates are the most radiosensitive (Hall *et al.*, 2012). Specifically, the p21 protein is induced by DEX in glioma cells, slows cell cycle progression and may confer cytoprotection (Naumann *et al.*, 1998; Glaser *et al.*, 2001; Ueda *et al.*, 2004) Further studies are warranted to more precisely establish interactions between DEX and these cell types and how these might influence the disease course.

In pursuit of alternatives to DEX, we demonstrated that short-term treatment with a low dose of VEGF antibody results in decrease in the total vessel area and the average vessel size, decreased leakage, and symptomatic edema control, permitting mice to be asymptomatic from intracranial tumors with larger tumor volumes. Moreover, VEGF

antibody treatment did not interfere with the efficacy of RT. Our data support the use of anti-VEGF agents as an alternative edema management strategy for glioblastoma patients. Of note, although the VEGF antibody bevacizumab did not prolong survival in newly diagnosed glioblastoma patients when added to standard of care, it nevertheless strongly prolonged progression-free survival which has been attributed in part to a confounding effect on imaging (Verhoeff *et al.*, 2009). Yet, these data altogether provide ample evidence that VEGF antagonism does not compromise the efficacy of RT in human patients in vivo. Moreover, a retrospective analysis of the AVAglio data demonstrated that patients with *IDH1* wild-type proneural glioblastoma might even derive a survival benefit from bevacizumab in that setting (Sandmann *et al.*, 2015).

In conclusion, given that controlled clinical trials to address the steroid question in glioblastoma are unlikely to be ever performed, we believe that our retrospective clinical data and corresponding data from animal models provides the so far strongest evidence against the traditional, often uncritical use of steroids in brain tumor patients.

LEGENDS

Figure 1. Corticosteroid use at the start of radiotherapy (RT) without or with TMZ is an independent marker of poor prognosis in human glioblastoma patients from three independent cohorts. Overall survival of (A) MSKCC, (B) EORTC 26981/22981 NCIC CE.3, (C) GGN patient cohorts.

Figure 2. **Association between steroid administration and outcome in the GGN cohort.** PFS by steroid use in all patients (A), PFS (B) and OS (C) for patients with RT only as initial treatment. PFS (D) and OS (E) for patients with RT/CT as initial treatment.

Figure 3. Association between steroid administration and outcome in the GGN cohort by extent of resection. PFS (A) and OS (B) by steroid use in GGN patients with gross total resection. PFS (C) and OS (D) by steroid use in GGN patients without gross total resection.

Figure 4. DEX but not anti-VEGFA antibody treatment decreases survival after RT. Mice with PDGF-driven gliomas were randomized into either DEX or untreated cohorts, and on the third day were further randomized into either **(A)** non-irradiated, **(B)** single dose, or **(C)** fractionated RT groups. DEX alone had no impact on survival, but decreased the efficacy of both single dose and fractionated RT. The cartoon at the bottom of each survival plot depicts the treatment schedule. **(D)** Kaplan-Meier survival curves for mice randomized into vehicle, B20-4.1.1 treatment, RT alone, or RT+B20.4.1.1 groups. Schematic illustrations of treatment paradigms for A-C are below and for D on the right together with experimental groups. p values were calculated using a Log-rank (Mantel-Cox) test, *p<0.05, **p<0.01, ****p<0.0001.

Figure 5. DEX-treated gliomas have down-regulation of cell cycle genes, which correlates with poor prognosis in the TCGA dataset. (**A**) 3D - PCA plot showing control- (black) and DEX- (red) treated samples (n=4 per each group). The axes of the plot denote the variation accounted for by each component. (**B**) Heat map and supervised clustering of arrays based on the most significant 25 probes, representing 19 genes. All of the genes are strongly down-regulated in DEX-treated samples. (**C**) Validation of seven DEX down-regulated genes by qRT-PCR. All samples are normalized to TBP expression levels. ****p <0.0001 for all comparisons, determined using one-way ANOVA. (**D**) Representative distribution of TCGA-samples by **A**bnormal **S**pindle-like, **M**icrocephaly-associated (ASPM) gene expression, based on z-scores normalized to diploid samples. Patients with elevated expression levels more than two standard deviations above the mean were considered minimally DEX-responsive. This process was repeated for the most significantly DEX-regulated genes. (**E**) Distribution of patients based on classifications as described above, showing the number of patients with high expression of 0-15 DEX-regulated genes. The graph (**F**) does not include the 423 (87%) patients who had no genes expressed above our threshold. This more clearly shows the distribution of minimally DEX-responsive patients. (F) Minimally DEX-responsive patients have significantly better overall survival rates (18.3 vs. 13.7 months). p values were calculated using a Log-rank (Mantel-Cox) test, **p<0.01, *p<0.05.

Figure 6. DEX suppresses proliferation of glioma cells in PDGF-driven murine gliomas. Representative bioluminescence images (BLI) of individual *Ntv-a/Ef-Luc* mice with PDGF-driven gliomas treated with either vehicle or with DEX at 10 mg/kg (**B**). DEX-treated mice received three total doses: at day 0 (immediately after BLI), day 1, and day 2 (1 hour pre-BLI). The bar graph shows that DEX treatment significantly decreased BLI output whereas vehicle treatment did not. Each group had n = 3 mice, values were normalized to day 0. (**C**) Representative tumor sections and (**D**) quantification of glioma proliferation using Olig2 expression as a glioma cell marker and PCNA as a proliferative marker. Data in upper panel are presented as the % of PCNA positive cells in total (based on nuclei count by DAPI per field) and the lower panel is the % of PCNA/Olig2 double positive cells in total PCNA positive cells per field. p values were calculated by paired ANOVA analyses within each group, **p<0.01, ***p<0.001 for **B** by unpaired Student's t-test, ****p<0001 for **D**. Scale bars: 50 μm in C.

Figure 7. Effects of anti-VEGF versus DEX treatment on blood vessel density, leakiness, tumor size and survival

(**A,C**) Kaplan-Meier survival curves for (**A**) DEX treatment vs. vehicle (n=7 and 7 for vehicle and DEX, respectively) and (**C**) B20-4.1.1 vs vehicle (n=14 and 15, respectively). Groups were matched based on initial asymptomatic T2-MRI tumor volume. (**B,D**) Representative images and quantification of T2-weighted MRI scans at time of symptom development for (**B**) vehicle- vs DEX treated mice (n=6 and 6, respectively) and (**D**) vehicle- and B20-4.1.1-treated mice (n=4 and 5, respectively). **(E)** Representative images and quantification (**F**) of CD31 staining of a tumor region after the administration of vehicle or DEX. (**G**)Representative images and quantification (**H**) of CD31 staining of a tumor region after the administration of vehicle or B20-4.1.1 **(I)** Illustration and representative images of a Hoechst dye leakage assay and functional vessel labeling with circulating FITC-conjugated lectin in vehicle- and a B20-4.1.1-treated tumors. (**F**) Corresponding quantification of Hoechst-positive area in B20-4.1.1-treated tumors compared to vehicle-treated tumors. p values were calculated using an unpaired Student's t-test, *p<0.05 **p < 0.01, ****p < 0.0001: Scale bars: 50 μm for A and C and 100 μm for E.

Figure 8. B20-4.1.1 decreases proliferation and increases cell death in murine PDGF-driven gliomas. **(A)** Representative tumor sections and (**B**) quantification bar graphs of glioma proliferation using Olig2 expression as a glioma cell marker and PCNA as a proliferative marker. There was a significant reduction in the proliferation of glioma cells after B20-4.1.1 treatment. **(C)** Representative images of Olig2 staining in tumor sections showing decreased staining in B20-4.1.1**-**treated mice compared to vehicle-treated mice. **(D)** Representative images of TUNEL staining in vehicle- and B20-4.1.1-treated tumors and **(E)** corresponding quantification of Olig2-positive area (F) and TUNEL-positive cells in response to B20-4.1.1 treatment. P values were calculated by an unpaired Student's t-test, *p < 0.05, ***p < 0.001, ****p<0.0001. Scale bars: 50 μm for A, C and D.

ACKNOWLEDGEMENTS

We would like to thank Paul Gambon and Dr. Xi Feng for technical assistance. We are grateful to Dr. Judy Drazba from the Imaging Core at the Lerner Research Institute for technical advices and to Dr. Grahame Kidd for confocal imaging. We are also grateful to the staff at the small-animal imaging core at CWRU. We are grateful to Dr. Jaekeun Park at small animal imaging core at Emory University School o Medicine for assistance with MRI scans. We acknowledge the support of all staff involved in EORTC 26981-22981 NCIC CE.3 and at the clinical sites of the German Glioma Network.

Research Support: NIH grants (ECH) RO1 CA100688, U54 CA163167, U54 CA143798, U01 CA141502-01; (TSJ) K08 CA163765, (KLP) MSTP GM07739, F31 NS076028. MC was supported by a MSKCC Brain Tumor Center Medical Student Summer Fellowship.

References

Becher OJ, Hambardzumyan D, Fomchenko EI, Momota H, Mainwaring L, Bleau AM*, et al.* Gli activity correlates with tumor grade in platelet-derived growth factor-induced gliomas. Cancer Res 2008; 68(7): 2241-9.

Eisenberg HM, Barlow CF, Lorenzo AV. Effect of dexamethasone on altered brain vascular permeability. Archives of neurology 1970; 23(1): 18-22.

Ellsworth S, Grossman SA. Comment on 'Dexamethasone exerts profound immunologic interference on treatment efficacy for recurrent glioblastoma'. Br J Cancer 2015; 113(11): 1632-3.

Feng X, Szulzewsky F, Yerevanian A, Chen Z, Heinzmann D, Rasmussen RD*, et al.* Loss of CX3CR1 increases accumulation of inflammatory monocytes and promotes gliomagenesis. Oncotarget 2015; 6(17): 15077-94.

Gerstner ER, Duda DG, di Tomaso E, Ryg PA, Loeffler JS, Sorensen AG*, et al.* VEGF inhibitors in the treatment of cerebral edema in patients with brain cancer. Nature reviews Clinical oncology 2009; 6(4): 229-36.

Glaser T, Wagenknecht B, Weller M. Identification of p21 as a target of cycloheximide-mediated facilitation of CD95-mediated apoptosis in human malignant glioma cells. Oncogene 2001; 20(35): 4757-67.

Gorlia T, van den Bent MJ, Hegi ME, Mirimanoff RO, Weller M, Cairncross JG*, et al.* Nomograms for predicting survival of patients with newly diagnosed glioblastoma: prognostic factor analysis of EORTC and NCIC trial 26981-22981/CE.3. Lancet Oncol 2008; 9(1): 29-38.

Grasso RJ, Johnson CE, Boler RK, Moore NA. Combined growth-inhibitory responses and ultrastructural alterations produced by 1,3-bis(2-chloroethyl)-1-nitrosourea and dexamethasone in rat glioma cell cultures. Cancer Res 1977; 37(2): 585-94.

Hall EJ, Giaccia AJ, Ovid Technologies Inc. Radiobiology for the radiologist. 7th ed. Philadelphia: Wolters Kluwer Health/Lippincott Williams & Wilkins; 2012. p. 576 p.

Hambardzumyan D, Amankulor NM, Helmy KY, Becher OJ, Holland EC. Modeling Adult Gliomas Using RCAS/t-va Technology. Translational oncology 2009; 2(2): 89-95.

Hambardzumyan D, Becher OJ, Rosenblum MK, Pandolfi PP, Manova-Todorova K, Holland EC. PI3K pathway regulates survival of cancer stem cells residing in the perivascular niche following radiation in medulloblastoma in vivo. Genes Dev 2008; 22(4): 436-48.

Hambardzumyan D, Gutmann DH, Kettenmann H. The role of microglia and macrophages in glioma maintenance and progression. Nat Neurosci 2015; 19(1): 20-7.

Helmy K, Halliday J, Fomchenko E, Setty M, Pitter K, Hafemeister C*, et al.* Identification of global alteration of translational regulation in glioma in vivo. PloS one 2012; 7(10): e46965.

Kamoun WS, Ley CD, Farrar CT, Duyverman AM, Lahdenranta J, Lacorre DA*, et al.* Edema control by cediranib, a vascular endothelial growth factor receptor-targeted kinase inhibitor, prolongs survival despite persistent brain tumor growth in mice. J Clin Oncol 2009; 27(15): 2542-52.

Kokunai T, Tamaki N. Relationship between expression of p21WAF1/CIP1 and radioresistance in human gliomas. Japanese journal of cancer research : Gann 1999; 90(6): 638-46.

Kostaras X, Cusano F, Kline GA, Roa W, Easaw J. Use of dexamethasone in patients with high-grade glioma: a clinical practice guideline. Current oncology 2014; 21(3): e493-503.
Kotsarini C, Griffiths PD, Wilkinson ID, Hoggard N. A systematic review of the literature on the effects of dexamethasone on the brain from in vivo human-based studies: implications for physiological brain imaging of patients with intracranial tumors. Neurosurgery 2010; 67(6): 1799-815; discussion 815.
Koutcher JA, Hu X, Xu S, Gade TP, Leeds N, Zhou XJ*, et al.* MRI of mouse models for gliomas shows similarities to humans and can be used to identify mice for preclinical trials. Neoplasia 2002; 4(6): 480-5.
Lu-Emerson C, Snuderl M, Kirkpatrick ND, Goveia J, Davidson C, Huang Y*, et al.* Increase in tumor-associated macrophages after antiangiogenic therapy is associated with poor survival among patients with recurrent glioblastoma. Neuro Oncol 2013; 15(8): 1079-87.
Naumann U, Durka S, Weller M. Dexamethasone-mediated protection from drug cytotoxicity: association with p21WAF1/CIP1 protein accumulation? Oncogene 1998; 17(12): 1567-75.
Nestler U, Winking M, Boker DK. The tissue level of dexamethasone in human brain tumors is about 1000 times lower than the cytotoxic concentration in cell culture. Neurological research 2002; 24(5): 479-82.
Ostrom QT, Gittleman H, Liao P, Rouse C, Chen Y, Dowling J*, et al.* CBTRUS statistical report: primary brain and central nervous system tumors diagnosed in the United States in 2007-2011. Neuro Oncol 2014; 16 Suppl 4: iv1-63.
Parr MJ, Manome Y, Tanaka T, Wen P, Kufe DW, Kaelin WG, Jr.*, et al.* Tumor-selective transgene expression in vivo mediated by an E2F-responsive adenoviral vector. Nat Med 1997; 3(10): 1145-9.
Piette C, Munaut C, Foidart JM, Deprez M. Treating gliomas with glucocorticoids: from bedside to bench. Acta neuropathologica 2006; 112(6): 651-64.
Powell SN, Abraham HE. The Biology of radioresistance: similarities, differences and interactions with drug resiastance. 1994; Multiple Drug Resistance in Cancer: Cellular, Molecular and Clinial Approaches eddited by Martin Clynes: 325-47.
Raslan A, Bhardwaj A. Medical management of cerebral edema. Neurosurgical focus 2007; 22(5): E12.
Reagan-Shaw S, Nihal M, Ahmad N. Dose translation from animal to human studies revisited. FASEB journal : official publication of the Federation of American Societies for Experimental Biology 2008; 22(3): 659-61.
Rovit RL, Hagan R. Steroids and cerebral edema: the effects of glucocorticoids on abnormal capillary permeability following cerebral injury in cats. Journal of neuropathology and experimental neurology 1968; 27(2): 277-99.
Sandmann T, Bourgon R, Garcia J, Li C, Cloughesy T, Chinot OL*, et al.* Patients With Proneural Glioblastoma May Derive Overall Survival Benefit From the Addition of Bevacizumab to First-Line Radiotherapy and Temozolomide: Retrospective Analysis of the AVAglio Trial. J Clin Oncol 2015; 33(25): 2735-44.
Shields LB, Shelton BJ, Shearer AJ, Chen L, Sun DA, Parsons S*, et al.* Dexamethasone administration during definitive radiation and temozolomide renders a poor prognosis in a retrospective analysis of newly diagnosed glioblastoma patients. Radiat Oncol 2015; 10: 222.

Stupp R, Hegi ME, Gorlia T, Erridge SC, Perry J, Hong YK*, et al.* Cilengitide combined with standard treatment for patients with newly diagnosed glioblastoma with methylated MGMT promoter (CENTRIC EORTC 26071-22072 study): a multicentre, randomised, open-label, phase 3 trial. The Lancet Oncology 2014; 15(10): 1100-8.
Stupp R, Mason WP, van den Bent MJ, Weller M, Fisher B, Taphoorn MJ*, et al.* Radiotherapy plus concomitant and adjuvant temozolomide for glioblastoma. N Engl J Med 2005; 352(10): 987-96.
Ueda S, Mineta T, Nakahara Y, Okamoto H, Shiraishi T, Tabuchi K. Induction of the DNA repair gene O6-methylguanine-DNA methyltransferase by dexamethasone in glioblastomas. Journal of neurosurgery 2004; 101(4): 659-63.
Uhrbom L, Nerio E, Holland EC. Dissecting tumor maintenance requirements using bioluminescence imaging of cell proliferation in a mouse glioma model. Nat Med 2004; 10(11): 1257-60.
Verhoeff JJ, van Tellingen O, Claes A, Stalpers LJ, van Linde ME, Richel DJ*, et al.* Concerns about anti-angiogenic treatment in patients with glioblastoma multiforme. BMC Cancer 2009; 9: 444.
Wang H, Li M, Rinehart JJ, Zhang R. Pretreatment with dexamethasone increases antitumor activity of carboplatin and gemcitabine in mice bearing human cancer xenografts: in vivo activity, pharmacokinetics, and clinical implications for cancer chemotherapy. Clin Cancer Res 2004; 10(5): 1633-44.
Weller M, Schmidt C, Roth W, Dichgans J. Chemotherapy of human malignant glioma: prevention of efficacy by dexamethasone? Neurology 1997; 48(6): 1704-9.
Wong ET, Lok E, Gautam S, Swanson KD. Dexamethasone exerts profound immunologic interference on treatment efficacy for recurrent glioblastoma. Br J Cancer 2015; 113(11): 1642.

Figure 1

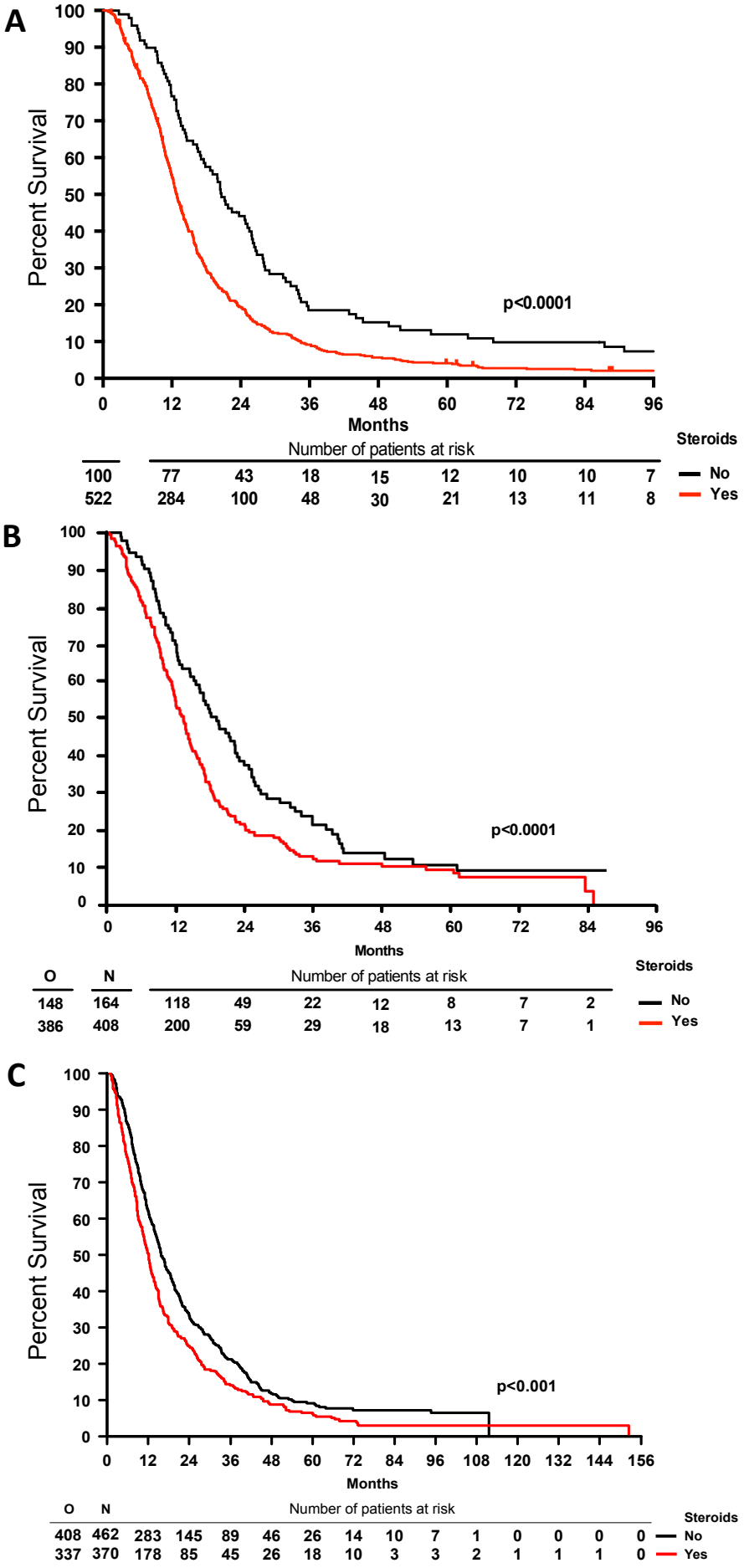
A
Percent Survival
100
90
80
70
60
50
40
30
20
10
0
p<0.0001
0 12 24 36 48 60 72 84 96
Months
Number of patients at risk
Steroids
100 77 43 18 15 12 10 10 7 No
522 284 100 48 30 21 13 11 8 Yes
B
Percent Survival
p<0.0001
0 12 24 36 48 60 72 84 96
Months
O N
Number of patients at risk
Steroids
148 164 118 49 22 12 8 7 2 No
386 408 200 59 29 18 13 7 1 Yes
C
Percent Survival
p<0.001
0 12 24 36 48 60 72 84 96 108 120 132 144 156
Months
O N
Number of patients at risk
Steroids
408 462 283 145 89 46 26 14 10 7 1 0 0 0 0 No
337 370 178 85 45 26 18 10 3 3 2 1 1 1 0 Yes

Figure 2

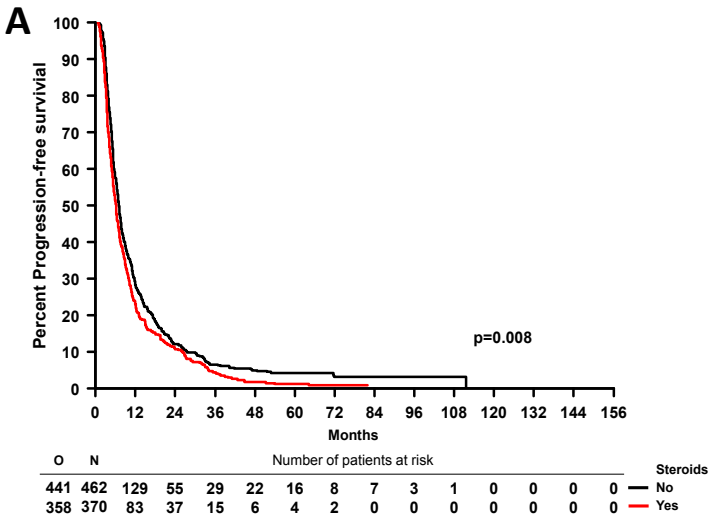
A
Percent Progression-free survivial
100
90
80
70
60
50
40
30
20
10
0
p=0.008
0 12 24 36 48 60 72 84 96 108 120 132 144 156
Months
O N Number of patients at risk
441 462 129 55 29 22 16 8 7 3 1 0 0 0 0
358 370 83 37 15 6 4 2 0 0 0 0 0 0 0
Steroids
No
Yes

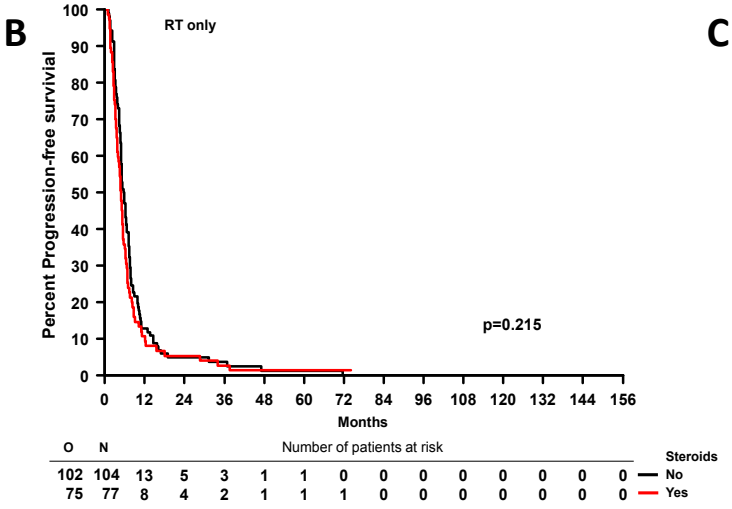
B
RT only
Percent Progression-free survivial
100
90
80
70
60
50
40
30
20
10
0
p=0.215
0 12 24 36 48 60 72 84 96 108 120 132 144 156
Months
O N Number of patients at risk
102 104 13 5 3 1 1 0 0 0 0 0 0 0 0
75 77 8 4 2 1 1 1 0 0 0 0 0 0 0
Steroids
No
Yes

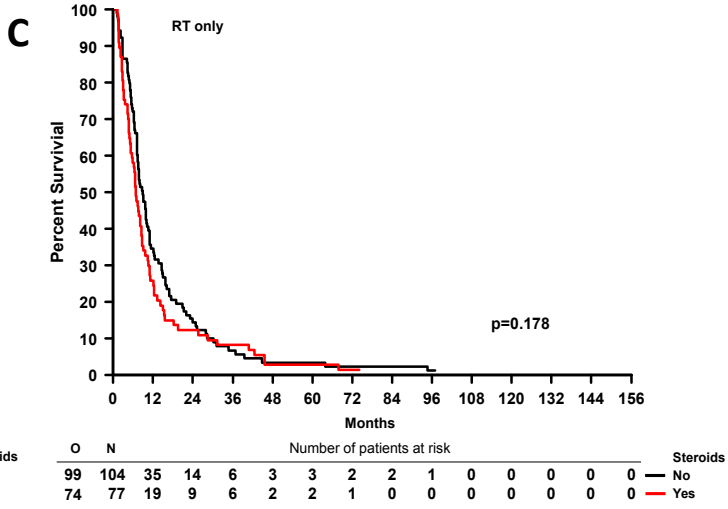
C
RT only
Percent Survivial
100
90
80
70
60
50
40
30
20
10
0
p=0.178
0 12 24 36 48 60 72 84 96 108 120 132 144 156
Months
O N Number of patients at risk
99 104 35 14 6 3 3 2 2 1 0 0 0 0 0
74 77 19 9 6 2 2 1 0 0 0 0 0 0 0
Steroids
No
Yes

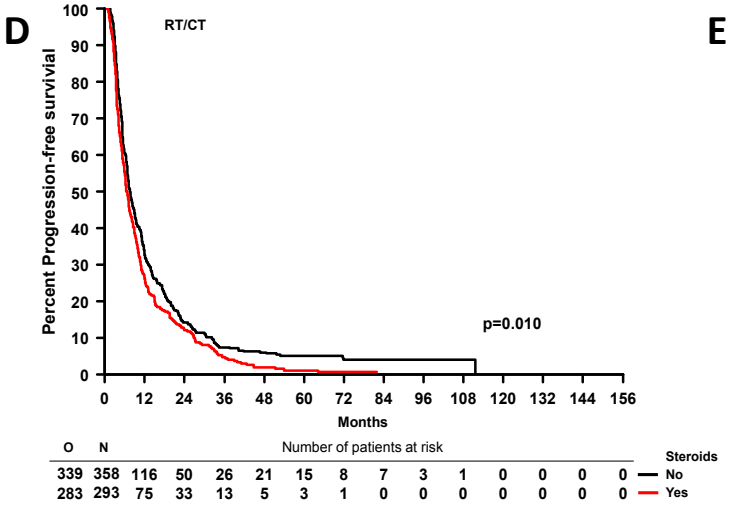
D
RT/CT
Percent Progression-free survivial
100
90
80
70
60
50
40
30
20
10
0
p=0.010
0 12 24 36 48 60 72 84 96 108 120 132 144 156
Months
O N Number of patients at risk
339 358 116 50 26 21 15 8 7 3 1 0 0 0 0
283 293 75 33 13 5 3 1 0 0 0 0 0 0 0
Steroids
No
Yes

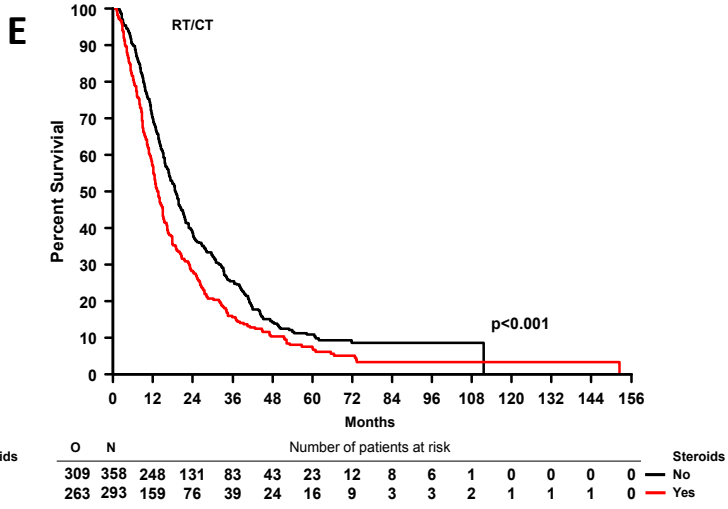
E
RT/CT
Percent Survivial
100
90
80
70
60
50
40
30
20
10
0
p<0.001
0 12 24 36 48 60 72 84 96 108 120 132 144 156
Months
O N Number of patients at risk
309 358 248 131 83 43 23 12 8 6 1 0 0 0 0
263 293 159 76 39 24 16 9 3 3 2 1 1 1 0
Steroids
No
Yes

Figure 3

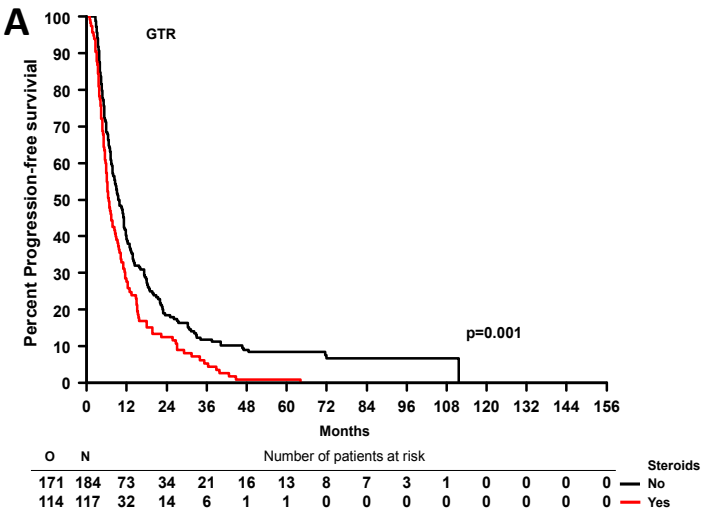
A
GTR
Percent Progression-free survivial
p=0.001
Months
Number of patients at risk
O N
171 184 73 34 21 16 13 8 7 3 1 0 0 0 0
114 117 32 14 6 1 1 0 0 0 0 0 0 0 0
Steroids
No
Yes

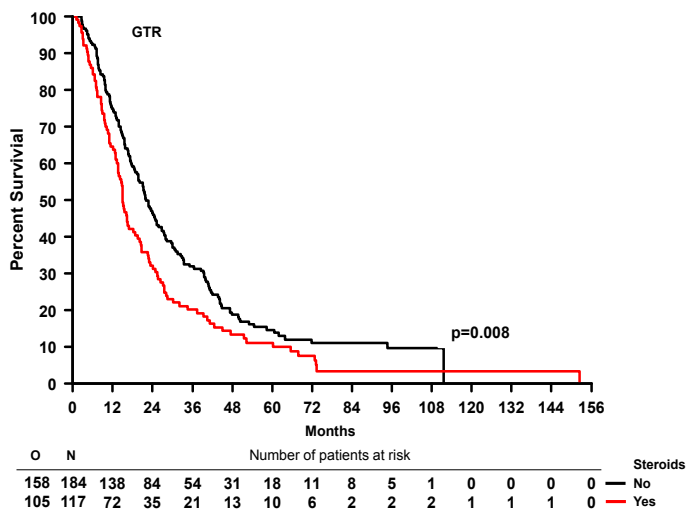
B
GTR
Percent Survivial
p=0.008
Months
Number of patients at risk
O N
158 184 138 84 54 31 18 11 8 5 1 0 0 0 0
105 117 72 35 21 13 10 6 2 2 2 1 1 1 0
Steroids
No
Yes

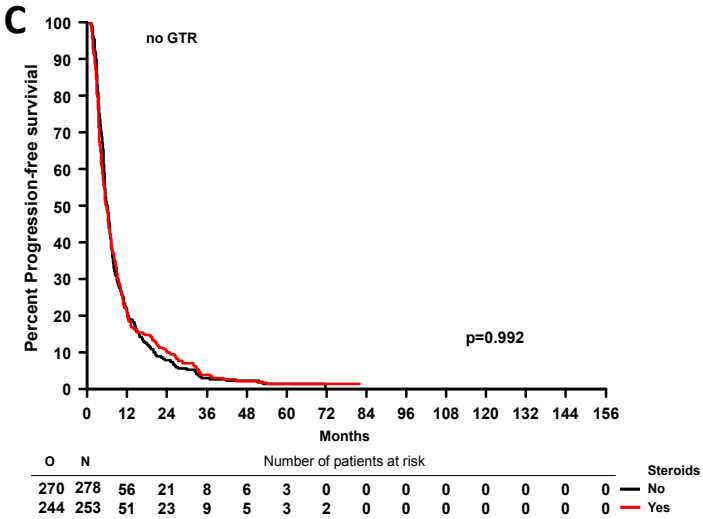
C
no GTR
Percent Progression-free survivial
p=0.992
Months
Number of patients at risk
O N
270 278 56 21 8 6 3 0 0 0 0 0 0 0 0
244 253 51 23 9 5 3 2 0 0 0 0 0 0 0
Steroids
No
Yes

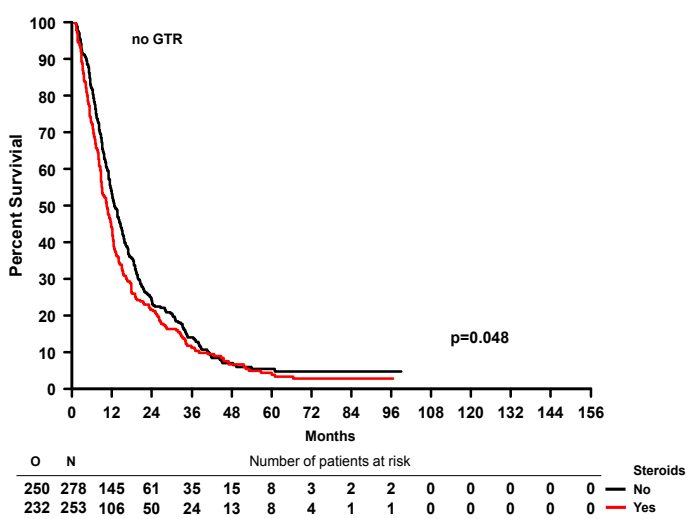
D
no GTR
Percent Survivial
p=0.048
Months
Number of patients at risk
O N
250 278 145 61 35 15 8 3 2 2 0 0 0 0 0
232 253 106 50 24 13 8 4 1 1 0 0 0 0 0
Steroids
No
Yes

Figure 5

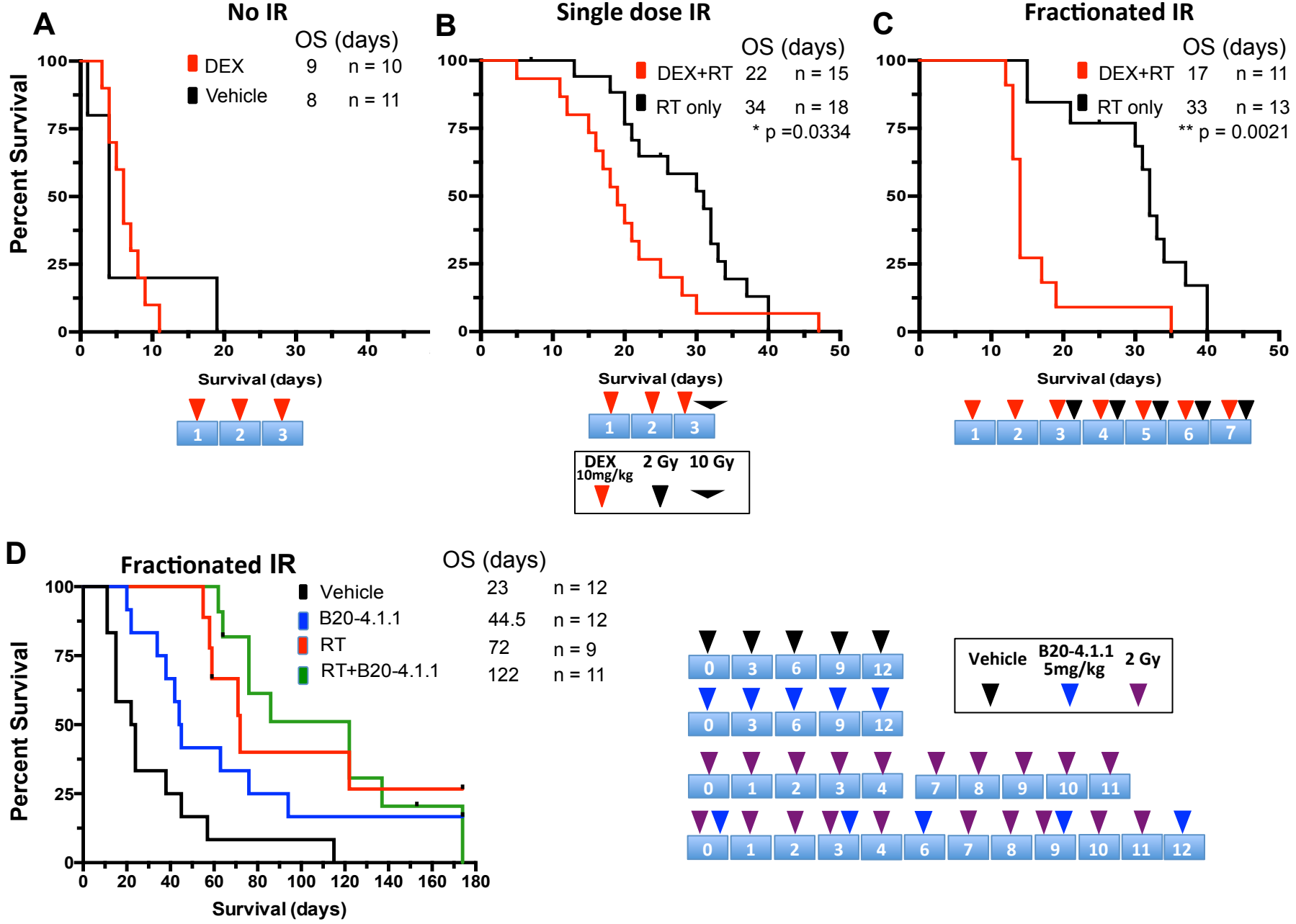
A
No IR
OS (days)
DEX 9 n = 10
Vehicle 8 n = 11
Percent Survival
Survival (days)
1 2 3
B
Single dose IR
OS (days)
DEX+RT 22 n = 15
RT only 34 n = 18
* p =0.0334
Survival (days)
1 2 3
DEX 10mg/kg
2 Gy
10 Gy
C
Fractionated IR
OS (days)
DEX+RT 17 n = 11
RT only 33 n = 13
** p = 0.0021
Survival (days)
1 2 3 4 5 6 7
D
Fractionated IR
Vehicle
B20-4.1.1
RT
RT+B20-4.1.1
OS (days)
23 n = 12
44.5 n = 12
72 n = 9
122 n = 11
Percent Survival
Survival (days)
Vehicle
B20-4.1.1 5mg/kg
2 Gy
0 3 6 9 12
0 3 6 9 12
0 1 2 3 4 7 8 9 10 11
0 1 2 3 4 6 7 8 9 10 11 12

Figure 5

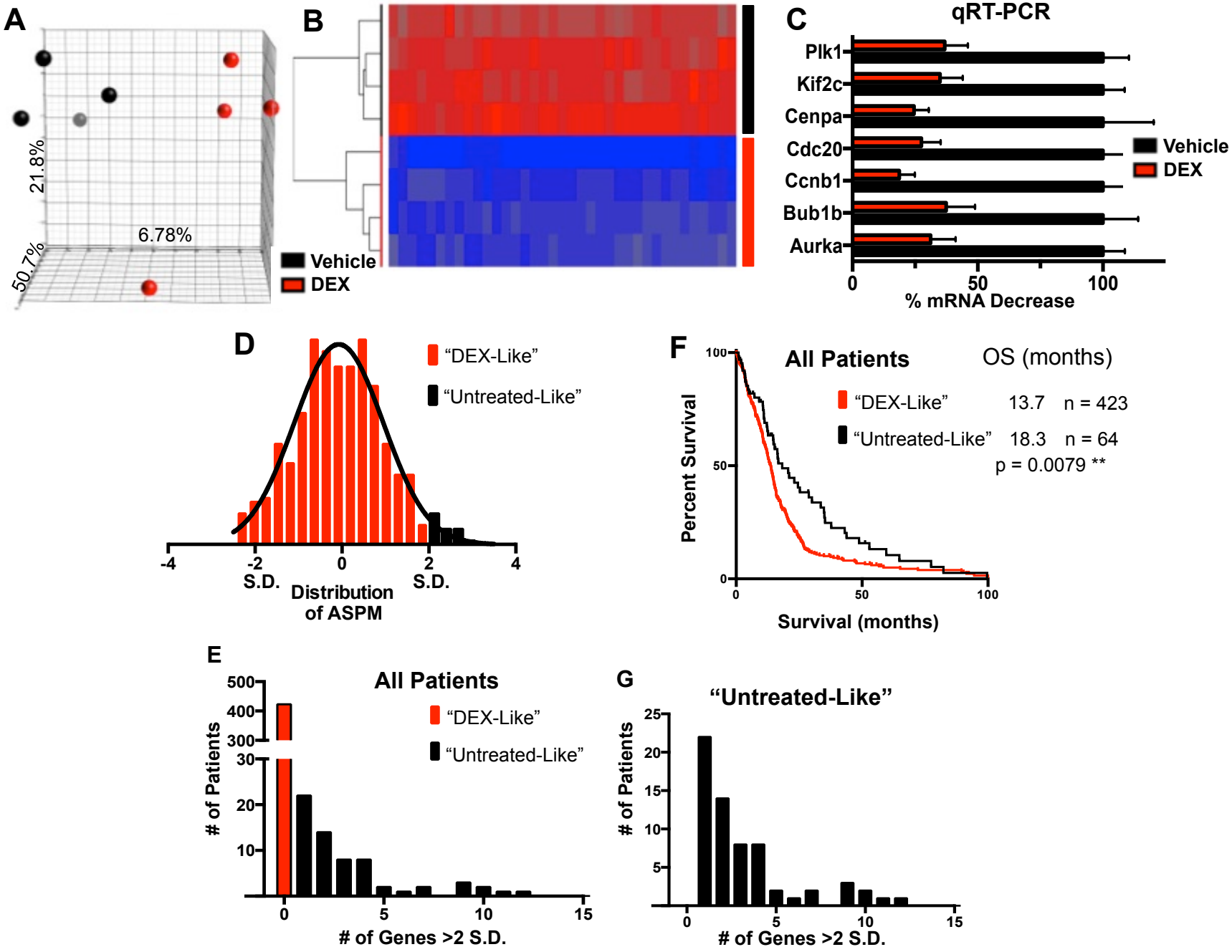
A
21.8%
6.78%
50.7%
B
Vehicle
DEX
C
qRT-PCR
Plk1
Kif2c
Cenpa
Cdc20
Ccnb1
Bub1b
Aurka
Vehicle
DEX
0
50
100
% mRNA Decrease
D
"DEX-Like"
"Untreated-Like"
-4
-2
0
2
4
S.D.
S.D.
Distribution of ASPM
F
All Patients
OS (months)
"DEX-Like" 13.7 n = 423
"Untreated-Like" 18.3 n = 64
p = 0.0079 **
Percent Survival
100
50
0
0
50
100
Survival (months)
E
All Patients
"DEX-Like"
"Untreated-Like"
# of Patients
500
400
300
30
20
10
0
5
10
15
# of Genes >2 S.D.
G
"Untreated-Like"
# of Patients
25
20
15
10
5
0
5
10
15
# of Genes >2 S.D.

Figure 6

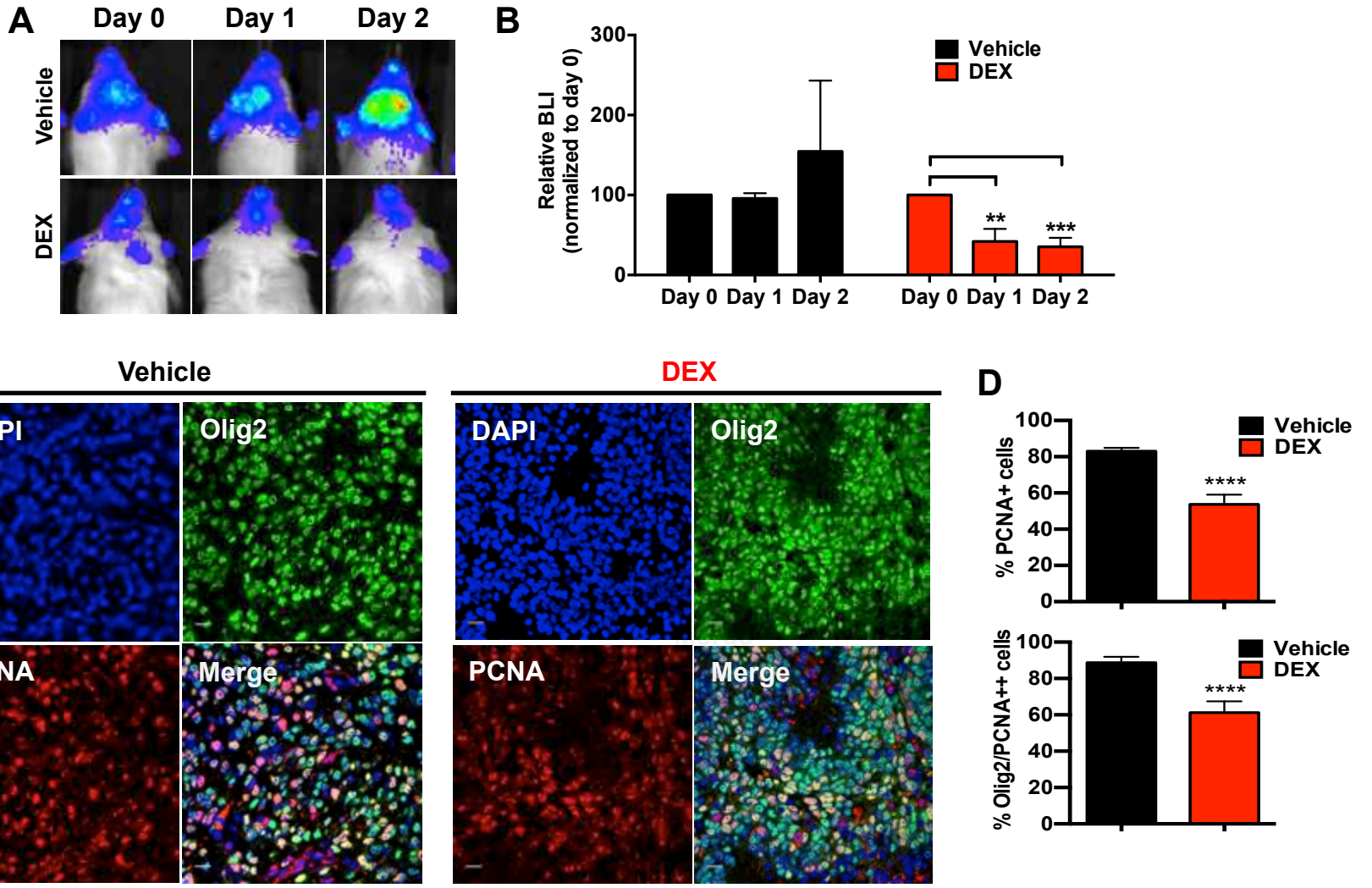
A
Day 0
Day 1
Day 2
Vehicle
DEX
B
Relative BLI
(normalized to day 0)
300
200
100
0
Vehicle
DEX
**
***
Day 0 Day 1 Day 2
Day 0 Day 1 Day 2
C
Vehicle
DEX
DAPI
Olig2
PCNA
Merge
DAPI
Olig2
PCNA
Merge
D
% PCNA+ cells
100
80
60
40
20
0
Vehicle
DEX
****
% Olig2/PCNA++ cells
100
80
60
40
20
0
Vehicle
DEX
****

Figure 7

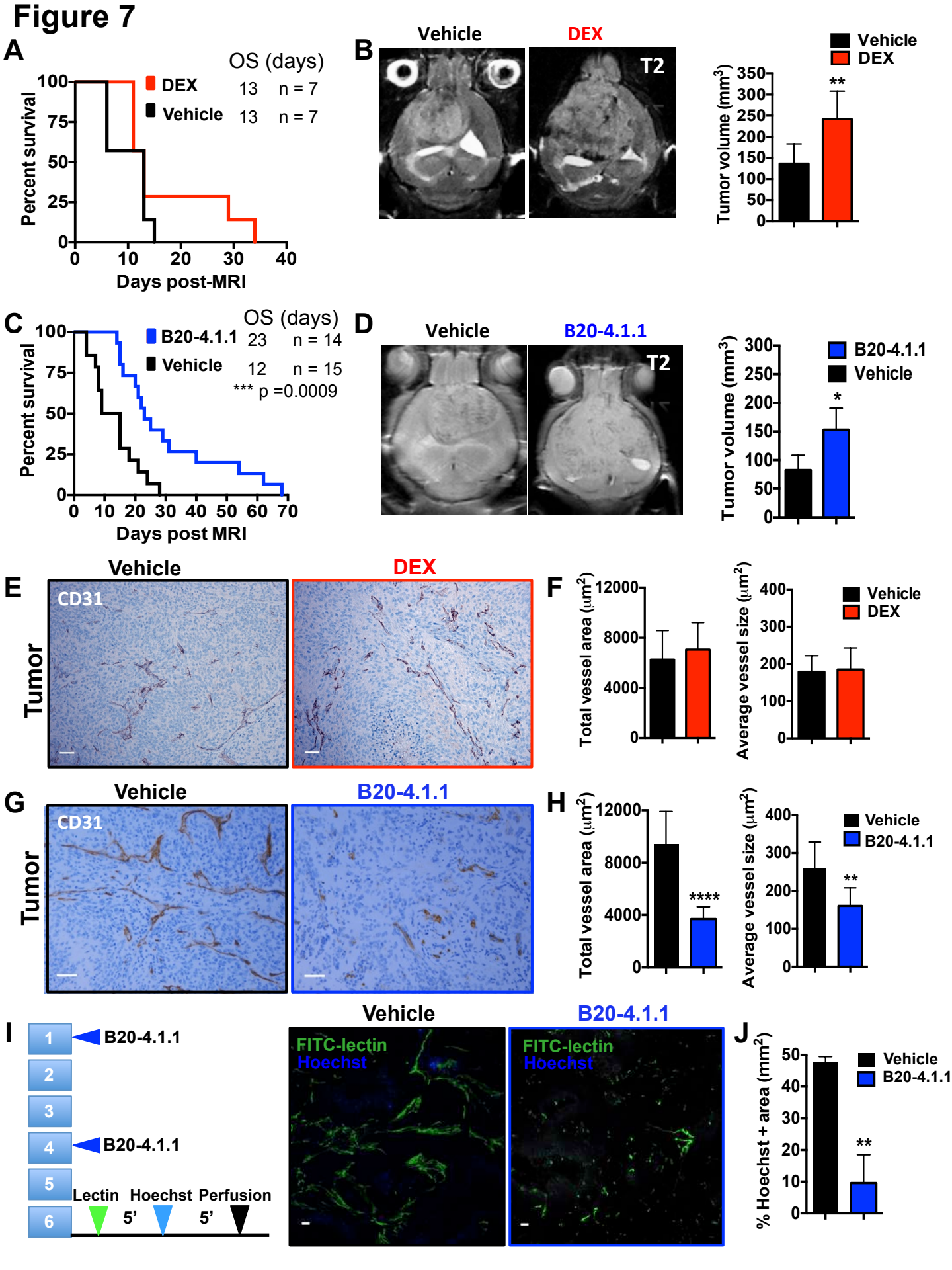
A
OS (days)
DEX 13 n = 7
Vehicle 13 n = 7
Percent survival
Days post-MRI
B
Vehicle
DEX
T2
Tumor volume (mm3)
C
OS (days)
B20-4.1.1 23 n = 14
Vehicle 12 n = 15
*** p =0.0009
Days post MRI
D
Vehicle
B20-4.1.1
E
Vehicle
DEX
CD31
Tumor
F
Total vessel area (μm2)
Average vessel size (μm2)
G
Vehicle
B20-4.1.1
H
I
B20-4.1.1
Lectin Hoechst Perfusion
5’ 5’
FITC-lectin
Hoechst
J
% Hoechst + area (mm2)

Figure 8

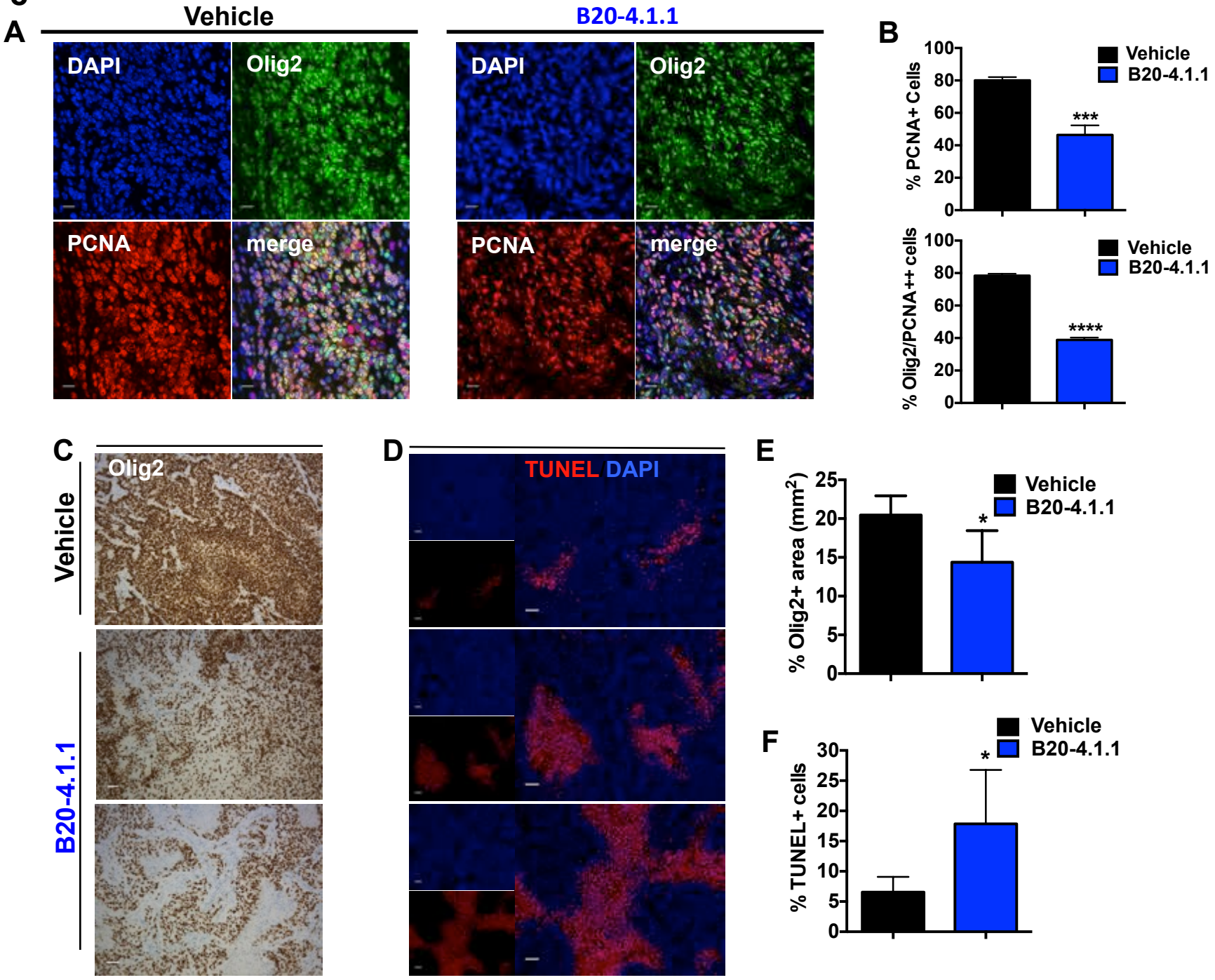
A
Vehicle
B20-4.1.1
DAPI
Olig2
PCNA
merge
B
% PCNA+ Cells
% Olig2/PCNA++ cells
Vehicle
B20-4.1.1
***
****
C
Olig2
D
TUNEL DAPI
E
% Olig2+ area (mm2)
F
% TUNEL+ cells
*

EXTENDED MATERIALS AND METHODS

Ethical statement

All animal experiments were conducted in strict accordance with the recommendations in the Guide for the Care and Use of Laboratory Animals of the National Institutes of Health and were approved by the Institutional Animal Care and Use Committees of the Lerner Research Institute (LRI), Cleveland Clinic and of Memorial Sloan-Kettering Cancer Center. The approved protocol numbers are 2013-1029 (LRI, last approved June 25, 2013), MSKCC-00-11-189 and Emory University 2003253 (EU last approved on September 15th 2015).

Cell cultures and transfections

DF-1 cells were purchased from ATCC (Manassas, VA). Cells were grown at 39°C in accordance with the manufacturer's instructions. Transfections with RCAS-PDGFB-HA and RCAS-sh-p53 were performed using a Fugene 6 transfection kit (# 11814443001; Roche, Mannheim, Germany).

Generation of RCAS/Tva system-based PDGFB-driven

Ntv-a/ink4a-arf-/- and *Gli-luc;Ntv-a;Ink4a-Arf$^{-/-}$* mice (6-8 weeks old) were sedated with intraperitoneal (i.p.) injections of ketamine (0.1 mg/g) and xylazine (0.02 mg/g). One microliter of 5 x 10^4 RCAS-PDGFB-HA-transfected DF-1 cell suspension was delivered from a Hamilton syringe with a 30-gauge needle attached to a stereotactic fixation device (Stoelting, Wood Dale, IL). For the *N-tva/*Ef-Luc, we injected 1 μL of a 1:1 mixture of 10^5 cells containing an equal mixture of RCAS-PDGFB-HA and RACS-shp53. Coordinates in the right frontal striatum were determined according to a mouse brain atlas[1] (coordinates from bregma: A/P 1.7 mm, Right- 0.5 mm, and depth 1.5 mm). Mice were sacrificed 4-6 weeks after injections, a time point after they had developed tumors. Mice were monitored and sacrificed when they displayed signs of tumor development (lethargy, weight loss).

Dexamethasone (DEX) treatment

Glioma-bearing mice received intraperitoneal (i.p.) injections of 10 mg/kg DEX (DexaJect, NDC #11695-4017-1, Butler Schein) and Sigma (D4902-25MG). Either upon becoming symptomatic

(Figure 4A,B,C) or based on MRI scans (Figure 6H,I), mice were treated with 10 mg/kg of DEX via i.p. injection for 3, 7 or 6 days. The DEX concentration in brain tissue is expected to be ~1 μM when mice are treated with 10 mg/kg [2,3].

B20-4.1.1 treatment

B20-4.1.1 (Genentech, CA) is an anti-VEGF-A monoclonal antibody (mAb) that inhibits VEGF-A interactions with VEGF receptors (VEGFR1 and VEGFR2) *in vitro*[4] and has been shown to inhibit VEGF-A-mediated angiogenesis *in vivo*[5,6]. For *in vivo* experiments, dilutions were made in sterile saline. For most mouse experiments, we used 5 mg/kg 2x/week dosing, or alternatively for short experiments we used 5 mg/kg for 1 week (only 2 doses). Vehicle-treated mice received the same volume of saline in 10 μl volume per g/body weight. For the survival experiment in Figure 5, B20-4.1.1 was used at a dose of 7.5 mg/kg.

For Figure 4D, four different treatment groups were included: vehicle-treated, B20-4.1.1 treatment alone (5 mg/kg, 2x/week), RT alone (20 Gy treatment, radiation was dosed at 2 Gy/day for five days followed by 2 days off and again dosed for another 5 days) and B20-4.1.1 treatment combined with RT simultaneously. During treatment, mice were weighed daily to assess toxicity from a single treatment or a combination of treatments, followed by weighing every other day to track the development of tumor-associated neurological signs (severe weight loss >15%, seizures, lethargy, lack of grooming), which was the end point of survival.

MRI scans

For T2-weighted MRI scans, each animal was first anesthetized with 1-2% isoflurane in oxygen and positioned at the isocenter of a 9.4T Bruker Biospec small animal MRI scanner (Bruker Inc., Billerica, MA) at the Center for Imaging Research at Case Western Reserve University (CWRU), Cleveland, OH for Figure 6G and H and 9.4T Bruker Biospec at Emory University small animal imaging core (Figure 6H,I) (Atlanta, GA). After initial localizer scans, a high-resolution coronal proton-density RARE (Rapid Acquisition with Relaxation Enhancement) acquisition was obtained for each animal (TR/TE = 5000/12 ms, resolution = 700 x 270 x 270 μm), slice thickness 0.7mm, 12 slices total . To acquire T1-contrast MRI scans, the animals were then removed from the scanner and injected with 100 μl of the contrast agent gadolinium (Magnevist, Bayer, #NDC 50419-188-01) intravenously (i.v.). Animals were then repositioned

within the scanner for a post-contrast T1-weighted spin echo scan (TR/TE = 1000/14 ms, resolution = 700 x 270 x 270 μm). The average total examination time for each animal, including both T2 and T1, was 30 to 35 min. Tumor boundaries were manually determined based on hypo-intense regions in T2-weighted images. Total volume was determined from multi-slice T2-weighted MR data. In this model, T2-weighted hypo-intensities have been previously confirmed by histology to correlate with tumor tissue.[7] Volumes of interest were contoured around the enhancing rim of tumors on the contrast-enhancing T1 images for volume measurements as described. [8] Tumor volume and gender were used to randomize mice into treatment and vehicle groups.

Hoechst dye assay

Tumor-bearing mice were treated with B20-4.1.1 or vehicle for 6 days (two dose of 5 mg/kg, 3 days apart). At post-treatment day 6, animals were i.v. injected with 50 μl of DyLight488-labeled Lectin (Vector, #DL-1174, 2 mg/ml). After 5 min, mice were i.v. injected with a 2 mg/ml (50 μl) aqueous solution of Hoechst 33342 (Sigma, #H6024). After 5 min, mice were euthanized and perfused with fresh 4% paraformaldehyde (PFA) solution (Electron Microscopy Sciences, #15714). The brain was extracted and fixed in 4% PFA overnight and then transferred to a 30% sucrose solution in PBS for at least 72 h. Brains were cut into 40 μm slices using a Leica SM2010 R microtome. For confocal microscopy (Leica CTR6500), slices were washed in PBS and mounted onto a glass slide with anti-fade mounting medium and further analyzed. For quantification, at least 5 representative 10X images per tumor were taken to obtain the average number of positive cells per tumor and areas positive for Hoechst were quantified using ImageJ. At least 3 tumors were included in the B20-4.1.1 and vehicle groups.

TUNEL assay

Terminal deoxynucleotidyltransferase-mediated dUTP-biotin nick end labeling (TUNEL) assays for optical microscopy were performed on 5 μm sections using a Terminal Transferase recombinant kit (Roche, #3333566). Fluorescent TUNEL assays were performed using the In Situ Cell Detection Kit, TMR red (Roche, #12156792910).

Tissue processing

Animals were sedated with i.p. injections of ketamine (0.1 mg/g) and xylazine (0.02 mg/g), perfused with ice-cold Ringer's solution, and sacrificed. Brains were fixed in 10% neutral-buffered formalin for 72 h at room temperature, processed in a tissue processer (Leica TP1050), embedded in paraffin, sectioned (5 μm), and slide-mounted for immunohistochemistry (IHC) and immunofluorescence staining. Sections were deparaffinized in Histo-Clear (Richard-Allan Scientific, Walldorf, Germany) and were passed through graded alcohols before staining with a hematoxylin and eosin (H&E) reagent.

Immunohistochemistry

IHC staining was performed using an automated staining processor (Ventana Discovery XT Roche Inc., Tucson, AZ). The following primary antibodies were used at the following dilutions: rabbit polyclonal anti-Iba1, 1:250 (Wako, #019-19741); rabbit polyclonal anti-Olig2, 1:250 (Millipore, #AB9610); mouse monoclonal anti-PCNA, 1:2000 (DAKO, #M0879); rabbit polyclonal anti-phospho-Histone H3, 1:500 (Millipore, #06-570); rat monoclonal anti-CD31, 1:50 (Dianova, #DIA 310); rabbit polyclonal anti-KI67, 1:100 (Vector Laboratories, #VP-K451) and rabbit polyclonal anti-cleaved caspase 3 1:100 (Cell Signaling, #9661). Nuclei were counterstained with hematoxylin. Slides were visualized using a Leica DM5500 B widefield microscope. For quantification, 5 representative 20X images were taken for each tumor to obtain the average number of positive cells per tumor and were quantified using ImageJ. For some quantification, slides were scanned using a Spectrum system from Aperio and analyzed using ImageScop v11.1.2.760 (Aperio). Tumor regions were selected based on H&E staining and percent positivity was based on the percentage of total nuclei that were deemed positive by pixel density.

Immunofluorescence

Paraffin-embedded sections (5 μm) were deparaffinized in Histo-Clear (Richard-Allan Scientific # 6901) and passed through graded alcohols. Next, we performed antigen retrieval with citric acid (vector lab #H-3300) in a boiling water bath for 15 min. After two washes in PBS and permeabilization in 0.3% triton in 0.1 M PBS for 45 min, sections were incubated in 0.1 M PBS containing 2% BSA, 5% NDS, and 0.1% Triton for 1 h at room temperature. For staining, sections were incubated with the following antibodies overnight at 4°C in PBS plus 1% BSA: rabbit polyclonal anti-Iba1, 1:200 (Wako Pure Chemicals, #019-19741); rabbit polyclonal anti-

Olig2, 1:200 (Millipore, #AB9610); rat monoclonal anti-CD31, 1:50 (Dianova, #DIA 310); mouse monoclonal anti-GFAP, 1:1000 (Merck Millipore, #MAB360);. Secondary antibodies were conjugated to different Alexa-Fluor dyes (488, 555, 568 and 647) and used at a dilution of 1:500 in PBS. Nuclear counterstaining was performed with DAPI (Sigma, #D9542). Slides were visualized using a Leica CTR6500 microscope. For quantification, at least 5 representative 20X images for each tumor were taken to obtain the average number of positive cells per tumor and were quantified using ImageJ.

Bioluminescence imaging (BLI)

Mice were anesthetized with 3% isoflurane. The hair covering the head was shaved before retro-orbital injection with 75 mg/kg body weight of D-luciferin (30 mg/ml dH_2O at 2.5 µl per gram mouse weight). One min after injection of D-luciferin, images were acquired for 5 min for *Gli-luc;Ntv-a;Ink4a-Arf*$^{-/-}$ and 15 min for *Nestin-tv-a;E2F1-Luc* mice with an IVIS 100 (Xenogen) imaging system. A photographic image was taken, onto which the pseudocolor image representing the spatial distribution of photon count was projected. A circular region (1.5 cm diameter) of interest (ROI) covering the tumor region was defined and used to quantify the bioluminescent signals in all experiments. All representative images were formatted using the same maximum and minimum threshold parameters. DEX-treated mice were treated immediately after imaging on Day 0, and subsequently were treated 1 h before imaging on days 1 and 2. BLI was also used for monitoring the response to treatment. Tumor growth was monitored every 5 days using BLI. As soon as tumor-bearing mice produced a signal equal to at least 10^3 photons/sec, they were randomized into different treatment or vehicle groups.

Quantification of total vessel area and average vessel size

CD31+ vessels were quantified by counting vessel numbers and using the freehand tool with ImageJ and Fiji software to determine total area covered by vessels-total vessel area (excluding lumens). Average vessel size was calculated from total area and vessel density per 20X field. At least five and up to 15 20X images were analyzed per tumor to obtain representative values per tumor sample.

Quantification of necrotic areas

Paraffin-embedded tumor sections were stained with H&E. Subsequently, slides were scanned using a Spectrum system from Aperio and analyzed using ImageScop v11.1.2.760 (Aperio). The tumor region, as well as regions of necrosis, were selected and the necrotic index was calculated according to the following formula; Necrotic index = Area of necrosis (μm^2)/Total area of tumor section (μm^2)[9].

Radiation treatment (RT)

Mice were lightly sedated with ketamine (0.1 mg/g) and xylazine (0.02 mg/g) and were irradiated using a Pantak X-RAD 320 x-ray unit (PXI, North Branford, CT). Only the head was irradiated; the rest of the mouse was shielded with a specialized lead jig. The total dose and schedules are described in detail in Figures 5.

Primary glioma cell cultures

Glioma-bearing mice were euthanized and transcardially perfused with ice-cold PBS. The tumor was grossly dissected and enzymatically digested in Hanks balanced salt solution containing 12% papain and 10 μg/ml DNase at 37˚C for 15 min, with subsequent inactivation using ovomucoid (1 mg/mL) (Worthington, Lakewood, NJ). The resulting single cell suspension was resuspended in DMEM media containing 10% FBS, 2mM L-glutamine, 100 units/mL penicillin, and 100 μg/mL streptomycin. In order to mimic *in vivo* conditions, the primary cultures were treated with physiologically relevant, low and high concentrations (i.e. 0.1, 1 and 10 μM = 39.5 ng/ml, 395 ng/ml and 3950 ng/ml) of DEX. The cultures used in these experiments were freshly isolated from tumors and passaged in serum a maximum of 5 times.

MTT assays

Cell viability was measured using MTT assays (Sigma No. M5655). Primary glioma cultures were seeded at a density of 1000 per well in 96-well plates. A 50 mM stock solution of DEX (Sigma D4902) was prepared by dissolving the drug in DMSO. Cells were allowed to attach overnight and DEX or vehicle control was added to the appropriate wells. After 3 days of drug exposure, MTT was added and allowed to incubate for 3 h. Afterwards, the media was aspirated and the purple formazan crystals were dissolved in 100 μl DMSO (Fisher). Absorbance was

measured at wavelengths of 570/690 nm using a FLx800 fluorescence microplate reader (BioTek Instruments, Inc.).

Cell cycle analysis

Primary glioma cultures were seeded at a density of 4000 cells/mL in 10 cm plates. Cells were allowed to attach to the plates overnight and then treated with DMSO or 0.1, 1 and 10 μM DEX for 3 days. After trypsinization and washing in ice-cold PBS, cells were fixed in ice-cold 70% ethanol for at least 1 h. Subsequently, cells were washed with PBS and stained with 0.05 mg/ml propidium iodide (PI) in the presence of 0.1 mg/ml RNase and then analyzed using a BD Accuri C6 flow cytometer. Quantification of different phases of the cell cycle (G0/G1, S, G2/M) was performed using Modfit LT.

Microarray analysis

Gliomas were grossly dissected from four untreated and four DEX-treated (3 days @ 10 mg/kg) mice. Upon dissection, tissue was flash-frozen in liquid nitrogen, homogenized, and dissolved in Trizol (Invitrogen, Carlsbad, CA). RNA was extracted and processed for Illumina mouse-ref 8 array platform. Array data were analyzed using Partek analysis software. ANOVA statistics were run to determine significantly altered genes. The DEX gene signature was generated using an unadjusted p-value of $p > 5x10^{-4}$. Gene lists were uploaded into Ingenuity Pathway Analysis (www.ingenuity.com) for analysis of relevant pathways.

qRT-PCR

Total RNA was extracted from control and DEX-treated mouse tumor samples using Trizol reagent (Invitrogen). The yield and purity of the RNA was confirmed using Nanodrop; ND-1000 V3, spectrophotometer. cDNA was synthetized using transcriptor first strand cDNA synthesis kit using 1 μg of RNA (Roche Applied Sciences, Indianapolis, MN). Primers were designed using the Roche Universal Probe Library. The following primers were used: *Aurka* 5′-TTGCAGACTTCGGGTGGT-3′ (forward) and 5′-TCCAGGGTGCCACACATT-3′ (reverse), *Bub1b* 5′-TTACGCCGTACGTGGAAGA-3′ (forward) and 5′-GCTCAATCTTGCATGGTGTC-3′ (reverse), *Ccnb1* 5′-TGCATTTTGCTCCTTCTCAA-3′ (forward) and 5′-CAGGAAGCAGGGAGTCTTCA-3′ (reverse), *cdc20* 5′-ACATCAAGGGCGCTGTCAAG-3′

(forward) and 5′-AATGTGCCGGTCACTGGT-3′ (reverse), *Cenpa* 5′-CAAGGAGGAGACCCTCCAG -3′ (forward) and 5′-TTCTGTCTTCTGCGCAGTGT-3′ (reverse), *Kif2c* 5′-CGAAGGAGGTACCACAAAAGG-3′ (forward) and 5′-TTCGGTCGTAAGGGAAGAAG-3′ (reverse), *Plk1* 5′-TTGTAGTTTTGGAGCTCTGTCG-3′ (forward) and 5′-AGTGCCTTCCTCCTCTTGTG-3′ (reverse), *TBP* 5′-GGCCTCTCAGAAGCATCACTA-3′ (forward) and 5′-GCCAAGCCCTGAGCATAA-3′ (reverse),

The housekeeping gene, TATA-binding protein (TBP), was used for normalization. The qRT-PCR was performed using a LC480 light cycler under the following conditions; activation cycle for 5 min at 95°C, followed by 50 cycles of amplification. Each amplification cycle started with an activation step for 5 min at 95°C, an annealing step for 30 sec at 60°C, and finally an extension step at 72°C for 10 sec.

TCGA analysis

Expression values for each gene of interest were obtained from the MSKCC computational biology cancer genomics portal (http://www.cbioportal.org/cgx/index.do) which has annotated TCGA data [10,11]. Survival data were obtained from the TCGA data portal (https://tcga-data.nci.nih.gov/tcga/).

Retrospective clinical analyses

A retrospective clinical analysis was performed with permission from the Institutional Review Board of MSKCC. Adult patients (>18 years old) at the time of histologic diagnosis of a glioblastoma who underwent external beam radiotherapy between 1998 and 2008 were eligible for the study. From initial 677 pathologically confirmed glioblastomas, 55 were excluded (17 patients ≤18 years of age, 1 patient with brainstem glioma, 10 patients missing decisive RPA information and 27 patients with unknown DEX status at start of RT).Patients were not eligible for the study if more than one of the clinical or treatment characteristics listed were missing from the medical records. Clinical characteristics of patients were recorded, including: age at diagnosis, Karnofsky performance score (KPS), mental status (mini-mental status from initial encounter or description of patient interaction from first encounter), neurologic functional

status (defined as "working" or "not working" at time of diagnosis, as described in the original RTOG RPA analysis), and duration of symptoms before diagnosis. Treatment characteristics were recorded, including: extent of surgery (biopsy, subtotal resection, or gross total resection), RT dose and fractionation, use of corticosteroids at the start of RT, and use of temozolomide during RT. Clinical and treatment characteristics were used to group patients according the Radiation Therapy Oncology Group recursive partitioning analysis (RTOG RPA) classification system[12,13]. Categorical multivariate cox regression models were constructed correlating RTOG RPA class, initial chemotherapy use, and baseline corticosteroid use with clinical outcomes.

In the retrospective clinical analysis of 573 patients from the EORTC 26981/22981 trial, correlation analyses of baseline steroid use and dose with outcomes were performed by univariate and multivariate Cox regression models. In the whole population, all models were stratified by treatment and all multivariate models were adjusted for main prognostic factors (age, extent of surgery, performance status). In this subgroup study, all analyses were performed at an exploratory 5% significance level. P-values higher than 5% but lower than 10% were considered as "borderline non-significant".

We also studied 832 patients with glioblastoma enrolled in the German Glioma Network (GGN) (www.gliomnetzwerk.de). Diagnosis for all patients was confirmed by central pathology review according to the WHO classification of tumors of the central nervous system. Inclusion criteria for this analysis were RT alone or RT plus chemotherapy (TMZ in all but 17 patients) as the first-line therapy as well as documentation about medication with steroids during radiotherapy (yes or no). Progression-free survival (PFS) was calculated from the day of first surgery until progression, death or the end of follow-up. Overall survival (OS) was calculated from the day of first surgery until death or the end of follow-up. Logrank tests were used to compare outcome data. Cox regression models were built to assess the independent association of steroid use with OS adjusted for relevant clinical parameters.

Statistical analysis

Graphs were created using GraphPad Prism 6 (GraphPad Software, San Diego, CA) and were

analyzed as noted in the figure legends. Cox proportional hazards analysis was performed in the survival package 'survival' version 2.36-10[14] in the R studio software[15]. In the retrospective clinical analysis of EORTC 26981/22981 trial, SAS 9.4 was used, in particular the PHREG procedure for Cox modeling. *=p<0.05, **=p<0.01, ***=p<0.001, no asterisks = not significant.

References

1. Keith B, Franklin G. The Mouse Brain in Steriotaxic Coordinates. San Diego 1997;Academic Press.
2. Reagan-Shaw S, Nihal M, Ahmad N. Dose translation from animal to human studies revisited. FASEB journal : official publication of the Federation of American Societies for Experimental Biology 2008;22:659-61.
3. Nestler U, Winking M, Boker DK. The tissue level of dexamethasone in human brain tumors is about 1000 times lower than the cytotoxic concentration in cell culture. Neurological research 2002;24:479-82.
4. Fuh G, Wu P, Liang WC, et al. Structure-function studies of two synthetic anti-vascular endothelial growth factor Fabs and comparison with the Avastin Fab. The Journal of biological chemistry 2006;281:6625-31.
5. Liang WC, Wu X, Peale FV, et al. Cross-species vascular endothelial growth factor (VEGF)-blocking antibodies completely inhibit the growth of human tumor xenografts and measure the contribution of stromal VEGF. The Journal of biological chemistry 2006;281:951-61.
6. Bagri A, Kouros-Mehr H, Leong KG, Plowman GD. Use of anti-VEGF adjuvant therapy in cancer: challenges and rationale. Trends Mol Med 2010;16:122-32.
7. Koutcher JA, Hu X, Xu S, et al. MRI of mouse models for gliomas shows similarities to humans and can be used to identify mice for preclinical trials. Neoplasia 2002;4:480-5.
8. McConville P, Hambardzumyan D, Moody JB, et al. Magnetic resonance imaging determination of tumor grade and early response to temozolomide in a genetically engineered mouse model of glioma. Clinical cancer research : an official journal of the American Association for Cancer Research 2007;13:2897-904.
9. Li L, Lin X, Staver M, et al. Evaluating hypoxia-inducible factor-1alpha as a cancer therapeutic target via inducible RNA interference in vivo. Cancer Res 2005;65:7249-58.
10. Cerami E, Gao J, Dogrusoz U, et al. The cBio cancer genomics portal: an open platform for exploring multidimensional cancer genomics data. Cancer discovery 2012;2:401-4.
11. Gao J, Aksoy BA, Dogrusoz U, et al. Integrative analysis of complex cancer genomics and clinical profiles using the cBioPortal. Science signaling 2013;6:pl1.
12. Curran WJ, Jr., Scott CB, Horton J, et al. Recursive partitioning analysis of prognostic factors in three Radiation Therapy Oncology Group malignant glioma trials. Journal of the National Cancer Institute 1993;85:704-10.
13. Scott CB, Scarantino C, Urtasun R, et al. Validation and predictive power of Radiation Therapy Oncology Group (RTOG) recursive partitioning analysis classes for malignant glioma patients: a report using RTOG 90-06. Int J Radiat Oncol Biol Phys 1998;40:51-5.

14. Borgan Ø. Modeling Survival Data: Extending the Cox Model. Terry M. Therneau and Patricia M. Grambsch, Springer-Verlag, New York, 2000. No. of pages: xiii + 350. ISBN 0-387-98784-3. Stat Med 2001;20:2053-4.
15. RStudio. RStudio: Integrated development environment for R Version 0.96.122 ed. Boston, MA.2012:Retrieved May 11, 2013.

Supplemental legends

SFigure 1. DEX-treatment decreases proliferation but does not enhance glioma cell death. A) Representative immunohistochemical staining for Ki67 in vehicle and DEX-treated mice. Corresponding bar graph shows that DEX-treatment induces significant decrease in proliferation compared to Vehicle-treated tumors. B) Representative immunohistochemical staining for cleaved caspase-3 (an apoptotic marker) and H&E in vehicle- and DEX-treated mice. Corresponding bar graphs show quantification of % of CC3+positive cells and necrotic index (Necrotic index = Area of necrosis (μm^2)/Total area of tumor section (μm^2)* per 40X field within the tumor). No differences were observed with DEX treatment. N = 5 for all samples, p values were calculated with a Student's t-test. Scale bars: 50 μm for A.

SFigure 2. DEX does not suppress proliferation *in vitro*. (**A**) *In vitro* MTT assay of three independent primary murine glioma cultures treated with 0.1, 1 and 10 μM of DEX did not show a reduction in cell proliferation. (**B**) *In vitro* cell cycle analysis of primary murine glioma cultures treated with 3 days of 0.1, 1 and 10 μM of DEX showed that DEX induced a slight but significant increase in the G1 population (from 50.97% in vehicle to 54.19 - 54.82% with DEX), with a corresponding decrease in the G2 population (from 34.45% in vehicle to 30.17 - 30.53% with DEX). However, the magnitude of these changes was not as large as anticipated based on the *in vivo* BLI and IHC responses. p values were calculated using a one-way ANOVA in comparison to DMSO, * p<.05, **p<.01, *** p<0.001.

SFigure 3. B20-4.1.1 treatment has no effect on non-tumor vasculature, decreases edema by T1-contrast MRI and increases myeloid cell infiltration in contrast to DEX. A) Representative images of CD31 staining of a non-tumor cortical area in vehicle- and B20-4.1.1-treated mice and corresponding graphs showing no significant differences in either total vessel area or average vessel size between B20-4.1.1- and vehicle-treated mice. **B)** Representative images of T1-contrast MRI scans of vehicle- and B20-4.1.1-treated mice. Graphs comparing tumor volumes according to T1-contrast MRI scans in vehicle- and B20-4.1.1-treated mice at the endpoint of survival, demonstrating a statistically significant difference in tumor size between vehicle- and B20-4.1.1-treated animals. **C)** Representative images of Iba1 staining for tumor-

associated microglia/macrophages in vehicle and B20-4.1.1-treated mice (upper panel) and vehicle and DEX treated tumors. Graphs comparing the total Iba1 positive areas in vehicles and B20-4.1.1 and DEX treated mice show that while there is significant increase in macrophage infiltration in B20-4.1.1 treated mice compare to vehicle, no significant difference was observed in DEX-treated compare to vehicle-treated mice. p values were calculated using an unpaired Student's t-test, *p<0.05 **p < 0.01, ****p < 0.0001: Scale bars: 50 μm for A and C.

SFigure 4. Olig2-positive tumor cells showed a significant increase in cell death in response to B20-4.1.1 treatment. (A) Representative images of tumor sections and **(B)** corresponding quantification of cell death by TUNEL staining in Olig2-positive gliomas and CD31-positive endothelial cell populations. While there were no significant differences in the percentage of cell death of CD31-positive endothelial cells, there was a significant increase in the percentage of cell death of Olig2-positive tumor cells. n = 4 and 5 for vehicle and B20-4.1.1, respectively. p values were calculated with an unpaired Student's t-test, *p < 0.05. Scale bars: 50 μm.

STable 1. Patient and treatment characteristics, categorized by use of DEX at the start of radiotherapy. A) The median survival of all patients was 13.6 months (0.76-116.6 months) and 595 of the patients (96%) have died at the time of analysis. The median overall survival was 18.7, 18.4, 11.8, and 5.1 months in RTOG RPA classes III, IV, V, and VI, respectively (p<0.0001). **B)** Multivariate COX regression analysis of glioblastoma patients treated at MSKCC, examining RTOG RPA Class, concurrent TMZ, and DEX at the start of radiotherapy.

STable 2. Patient and treatment characteristics, categorized by use of DEX at the start of radiotherapy for GGN (A) and EORTC (B).

STable 3. A) PFS and OS in the GGN cohort by steroid use. B) Multivariate analysis of the association of steroid administration and outcome in the GGN cohort

STable 4. Genes and top predicted cellular functions and canonical pathways of DEX regulated gene set.. **A)** The 25 most significantly changed probes on an illumina mouse-ref-8 array. The gene list is based on a greater than 1.5 fold change, with an ANOVA p value <

0.0005. This list was generated using Partek Genomics Suite array analysis software (v6.6)**. B) Gene ontology analysis of DEX-regulated genes.** The top 5 most enriched predicted cellular function and canonical pathways, based on the 19 DEX-regulated genes.

Supplemental Figure 1

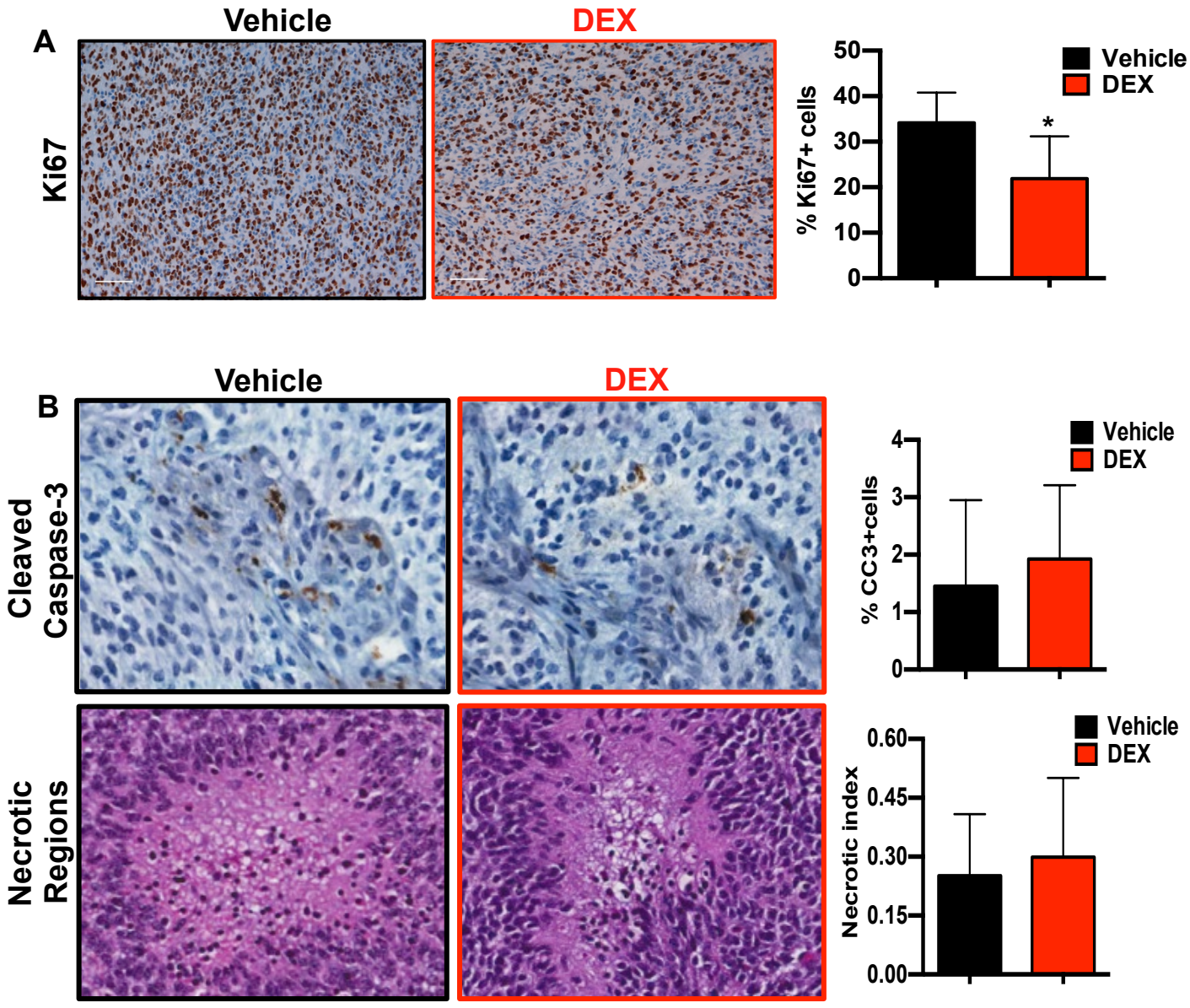

Supplemental Figure 2

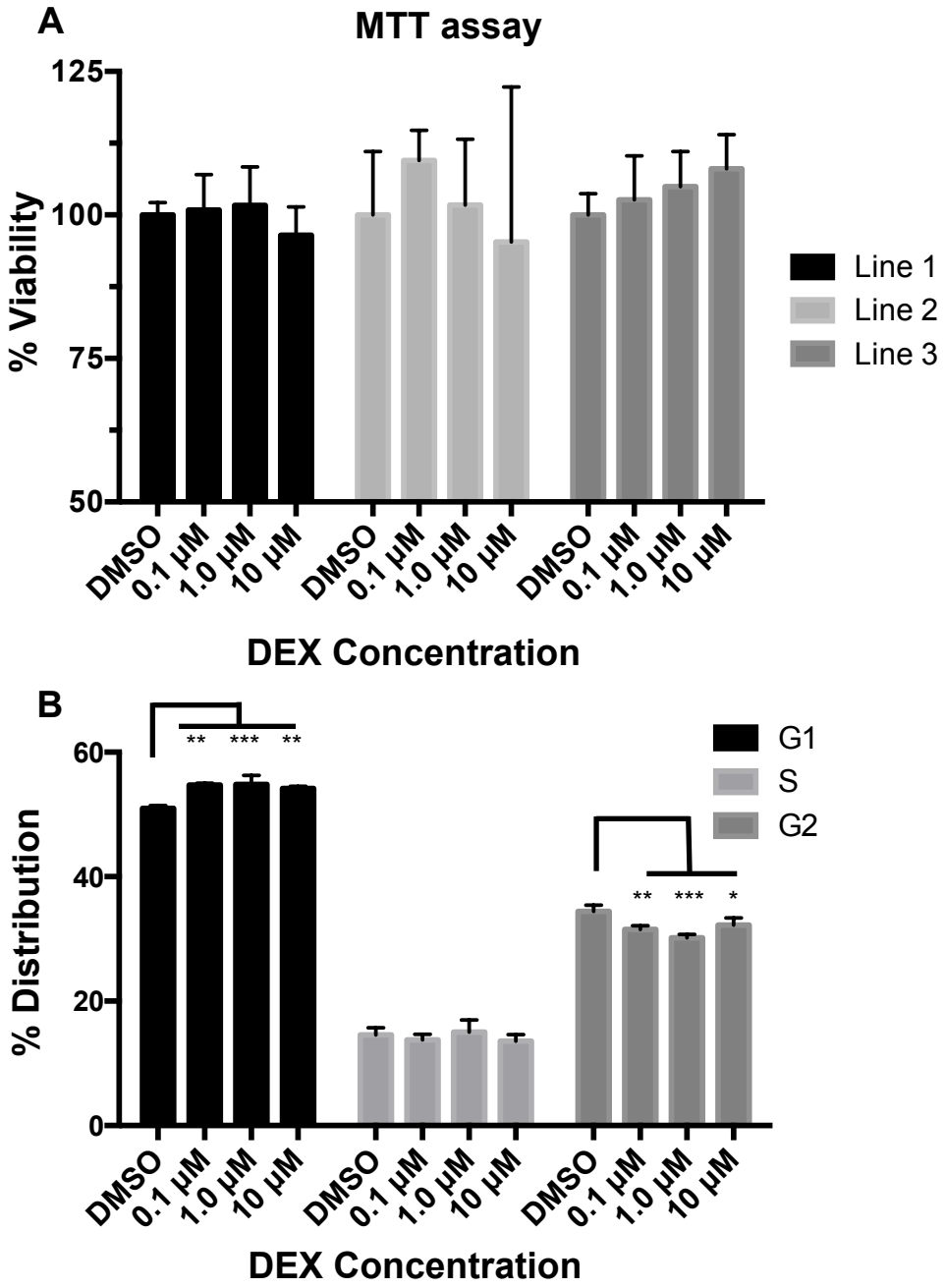

Supplemental Figure 3

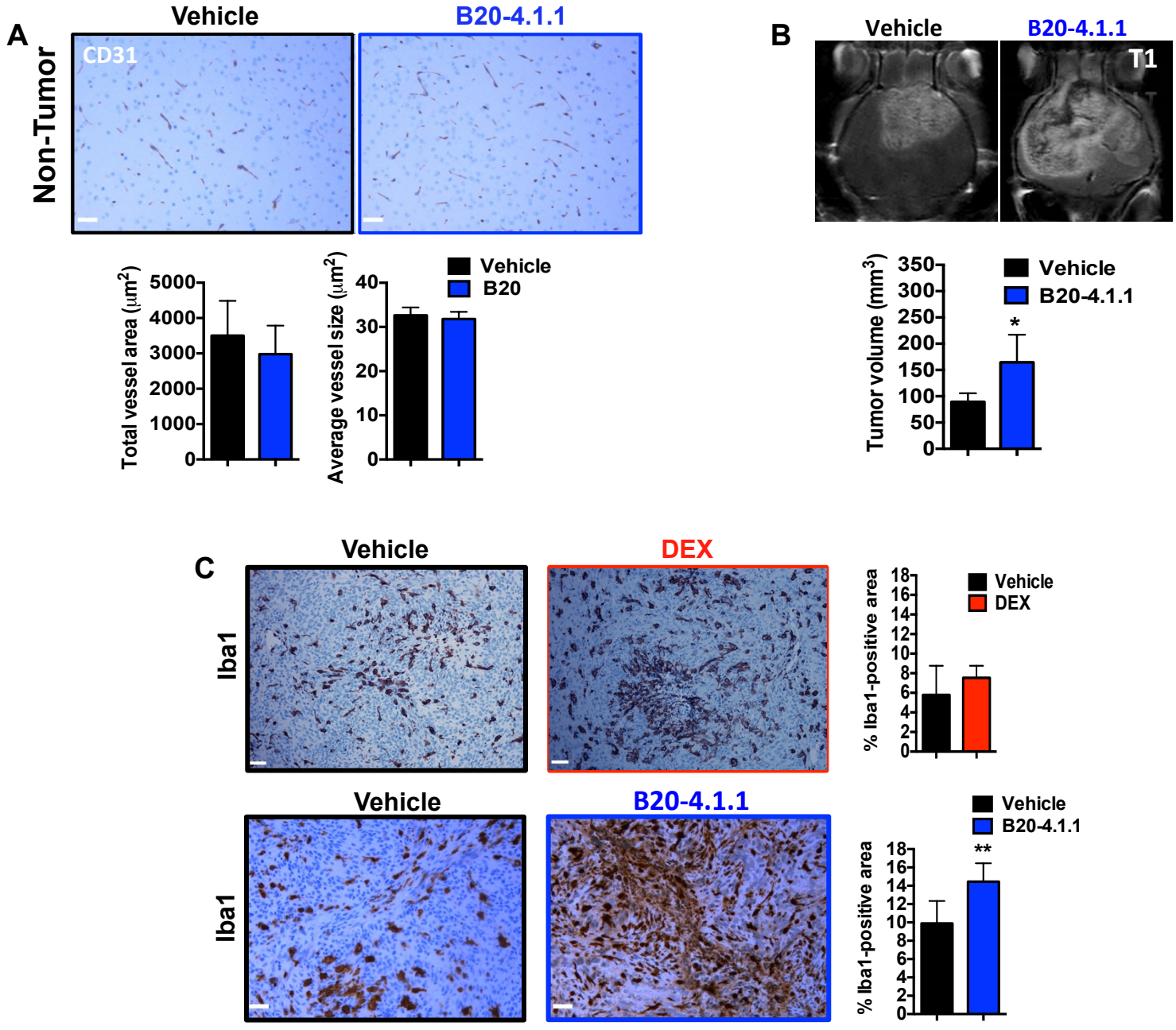

Supplemental Figure 4

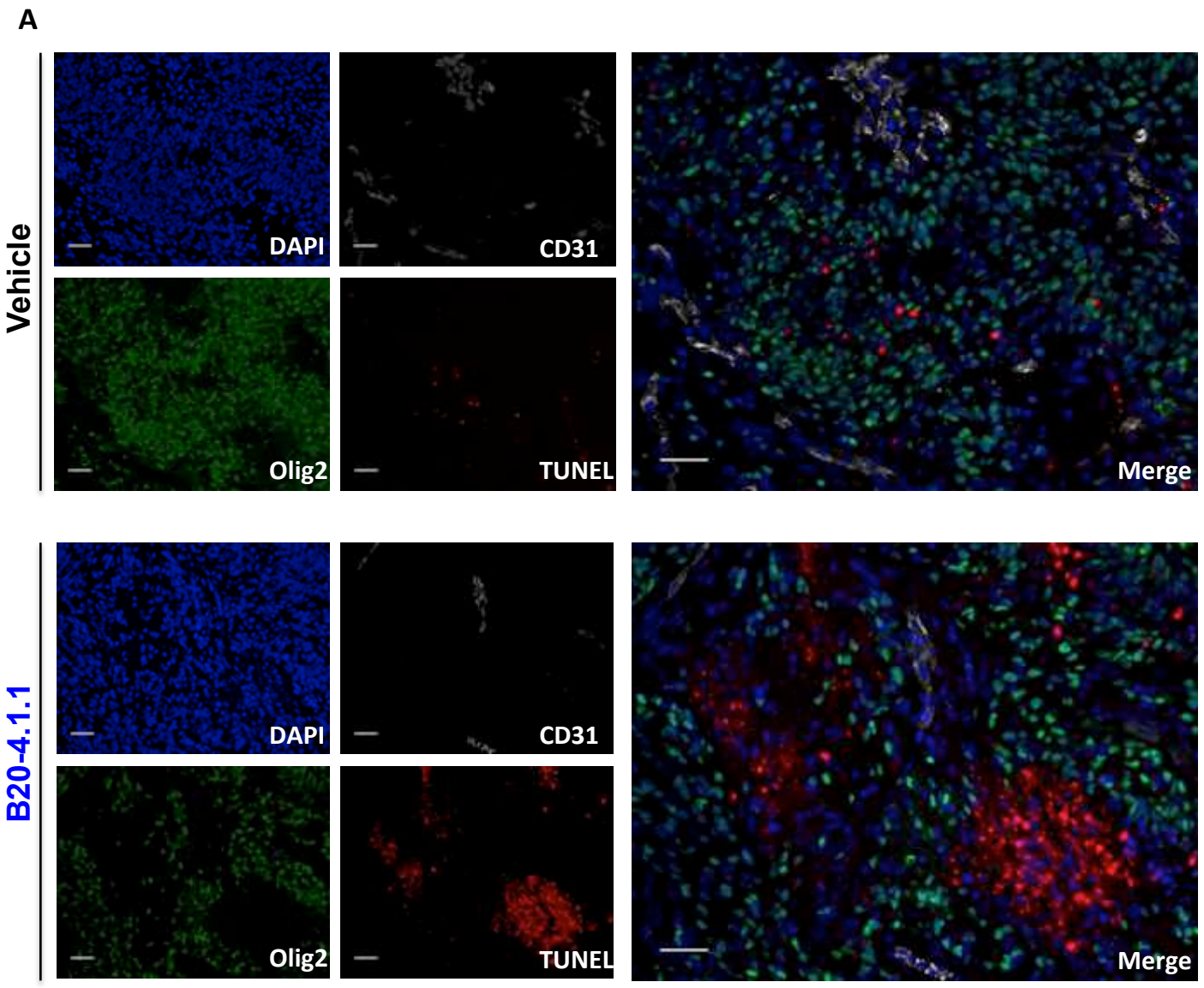

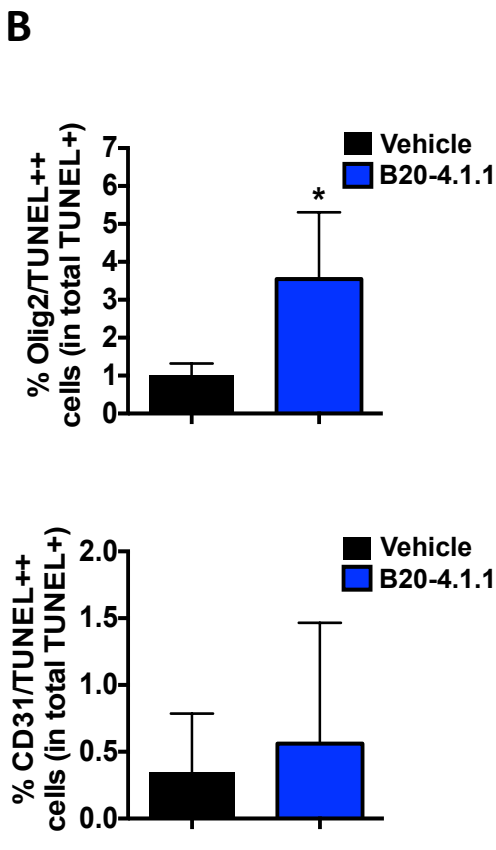

Table S1. Patient and treatment characteristics with or without DEX at the start of radiotherapy

A

Characteristic		N = 522 (84%) +Steroid	N= 100 (16%) -Steroid	p value^
Sex n (%)				
	M	326 (62.5%)	70 (70%)	0.1505
	F	196 (37.5%)	30 (30%)	
Age, y				
	Median	59	56	
Age, n (%)				
	<50	130 (24.9%)	27 (27%)	0.7063
	≥50	392 (75.1%)	73 (73%)	
KPS, n (%)				
	≥90	201 (38.5%)	68 (68%)	< 0.0001
	≥70 - <90	231 (44.3%)	28 (28%)	
	<70	90 (17.2%)	4 (4%)	
Mental Satus, n (%)				
	Normal	376 (72%)	85 (85%)	0.0207
	Abnormal	140 (26.8%)	15 (15%)	
	Data Missing	6 (1.1%)	0 (0%)	
Symptom Length				
	<12 wk	405 (77.6%)	76 (76%)	0.7285
	≥12 wk	117 (22.4%)	24 (24%)	
Neurologic functional status, n (%)				
	Working	162 (31%)	57 (57%)	< 0.0001
	Not Working	357 (68.4%)	43 (43%)	
	Data Missing	3 (0.6%)	0 (0%)	
Surgical Extent				
	Biopsy	97 (18.6%)	9 (9%)	0.0032
	Resection			
	STR	231 (44.3%)	37 (37%)	
	GTR	194 (37.2%)	54 (54%)	
Radiation Dose				
	>54.4 Gy	407 (78%)	90 (90%)	0.0019
	≤54.4	105 (20.1%)	6 (6%)	
	Data Missing	10 (1.9%)	4 (4%)	
RPA Class				
	Class 3	72 (13.8%)	23 (23%)	0.0004
	Class 4	145 (27.8%)	40 (40%)	
	Class 5	243 (46.6%)	34 (34%)	
	Class 6	62 (11.9%)	3 (3%)	
Concurrent Chemotherapy				
	TMZ	166 (31.8%)	46 (46%)	0.1381
	No TMZ	359 (67.5%)	51 (56.7%)	

^p value calculated using Chi squared test
KPS - Karnofsky Performance Status; STR - Subtotal Resection
GTR - Gross Total Resection, RTOG – Radiation Therapy Oncology Group
RPA - Recursive Partitioning Analysis; TMZ - Temozolomide

B

Cox proportional multivariate hazards analysis of ptient prognostic survival factors			
Variables	***p* value**	**HR**	**95% CI**
Dexamethasone	p = 0.00034	1.512	1.2058 - 1.8960
RTOG RPA Class	p < 0.0001	1.5461	1.3989 - 1.7088
Temozolomide	p = 0.00096	0.749	0.6312 - 0.8892

HR = hazard ratio CI = confidence interval

RTOG - Radiation Therapy Oncology Group
RPA - Recursive Partitioning Analysis

Table S2. Patient and treatment characteristics with or without DEX at the start of radiotherapy in EORTC (A) and GGN (B)

A

Characteristics	Steroids at baseline			Total (N=573)
	Missing N=1 (0.17%)	No N=164 (28.6%)	Yes N=408 (71.2%)	
Treatment				
RT	1 (100.0)	70 (42.7)	215 (52.7)	286 (49.9)
TMZ/RT	0 (0.0)	94 (57.3)	193 (47.3)	287 (50.1)
WHO Performance Status				
0	0 (0.0)	80 (48.8)	143 (35.0)	223 (38.9)
>0	1 (100.0)	84 (51.2)	265 (65.0)	350 (61.1)
Extent of surgery				
Biopsy	0 (0.0)	8 (4.9)	85 (20.8)	93 (16.2)
Partial Resection	0 (0.0)	65 (39.6)	189 (46.3)	254 (44.3)
Complete Resection	1 (100.0)	91 (55.5)	134 (32.8)	226 (39.4)
Age (continuous)				
Median	62.4	54.0	56.7	55.8
Range	62.4 - 62.4	19.0 - 70.8	18.6 - 70.5	18.6 - 70.8
N obs	1	164	408	573
Age (class)				
<=50	0 (0.0)	23 (14.0)	41 (10.0)	64 (11.2)
51-60	0 (0.0)	99 (60.4)	240 (58.8)	339 (59.2)
>60	1 (100.0)	42 (25.6)	127 (31.1)	170 (29.7)
last daily dose administered (mg)				
Median			8.0	8.0
Range			1.0 - 160.0	1.0 - 160.0
N obs	0	0	397	397
Tercile1				1-4
Median			4	4
Range			1-4	1-4
Tercile2				
Median			8	8
Range			5-10	5-10
Tercile3				
Median			16	16
Range			**12-160**	**12-160**

B

Characteristics	Steroids N=370 (44.5%)	No Steroids N=462 (55.5%)	p-value
Gender			
Male	213 (57.6%)	284 (61.5%)	0.254
Female	157 (42.4%)	178 (38.5%)	
Age, y			
Median (range)	63 (19 - 83)	60 (22 - 86)	0.194
≤60 y	158 (42.7%)	233 (50.4%)	
>60 y	212 (57.3%)	229 (49.6%)	
KPS			
<70	28 (7.6%)	22 (4.8%)	0.238
70-80	180 (48.6%)	233 (50.4%)	
≥90	162 (43.8%)	207 (44.8%)	
Surgical Extent			
biopsy	92 (24.9%)	72 (15.6%)	0.001
partial	48 (13.0%)	43 (9.3%)	
subtotal	113 (30.5%)	163 (35.3%)	
total	117 (31.6%)	184 (39.8%)	
Radiation Dose			
≤54 Gy	43 (13.2%)	37 (9.8%)	0.152
>54 Gy	282 (86.8%)	341 (90.2%)	
Data Missing	45	84	
Therapy			
RT	77 (20.8%)	104 (22.5%)	0.555
RT+CT	293 (79.2%)	358 (77.5%)	

Table S3. A) PFS and OS in the GGN cohort by steroid use. B) Multivariate analysis of the association of steroid administration and outcome in the GGN cohort.

A

	N (events)	PFS Median in months (95% CI) Events	PFS Median in months (95% CI) Events	HR, p value	OS Median in months (95% CI) Events	OS Median in months (95% CI) Events	HR, p value
Steroids		-	+		-	+	
Events							
All patients & events	832	7.0 (6.5-7.6) 441/462	6.1 (5.5-6.8) 358/370	1.21 0.008	15.7 (14.0-17.4) 408/462	12.1 (10.9-13.2) 337/370	1.32 <0.001
RT only	181	5.6 (4.8-6.5) 102/104	4.9 (4.2-5.6) 75/77	1.21 0.215	8.8 (7.1-10.5) 99/104	6.8 (5.7-8.0) 74/77	1.23 0.178
RT/CT	651	7.5 (6.6-8.5) 339/358	6.7 (5.9-7.5) 283/293	1.23 0.010	18.8 (16.8-20.7) 309/358	13.3 (11.7-14.9) 263/293	1.37 <0.001
GTR	301	9.5 (7.7-11.4) 171/184	6.7 (5.6-7.7) 114/117	1.51 0.001	22.1 (18.7-25.5) 158/184	15.0 (13.2-16.8) 105/117	1.40 0.008
No GTR	531	6.1 (5.3-6.9) 270/278	5.6 (4.8-6.4) 244/253	1.00 0.992	12.8 (11.1-14.4) 250/278	10.4 (8.7-12.0) 232/253	1.12 0.048
GTR							
RT only	51	5.8 (3.8-7.7) 33/34	5.4 (3.7-7.2) 17/17	1.05 0.863	9.9 (8.0-11.8) 32/34	10.9 (6.0-15.7) 17/17	1.20 0.539
RT/CT only	250	11.1 (9.3-13.0) 138/150	6.7 (5.1-8.3) 97/100	1.60 <0.001	24.5 (20.3-28.7) 126/150	15.3 (13.4-17.2) 88/100	1.47 0.006
No GTR							
RT only	130	5.3 (4.2-6.4) 69/70	4.5 (3.3-5.6) 58/60	1.24 0.239	8.0 (6.2-9.8) 67/70	6.4 (4.8-8.0) 57/60	1.20 0.320
RT/CT only	401	6.4 (5.5-7.3) 201/208	6.5 (5.3-7.6) 186/193	0.98 0.844	15.2 (13.1-17.3) 183/208	12.1 (10.7-13.4) 175/193	1.23 0.048

B

Factor	HR	95% CI	P value
Steroids Yes vs. no (ref.)	1.18	1.02 - 1.37	0.024
Therapy RT vs. RT/CT (ref.)	1.75	1.47 - 2.09	<0.001
Resection No gross total vs. gross total (ref.)	1.59	1.36 - 1.85	<0.001
Age >60 vs. ≤ 60 (ref.)	2.07	1.78 - 2.41	<0.001
KPS ≤ 80 vs. >80 (ref.)	1.17	1.00 - 1.36	0.041

Table S4. Genes and top predicted cellular functions and canonical pathways of DEX regulated gene set.

A The 25 most significantly changed probes on illumina mouse-ref-8 array. Gene list based on a greater than 1.5 fold change, with an ANOVA p value > 0.0005.

Illumina Probeset ID	SYMBOL	ANOVA p-value	Fold-Change (Dex vs. Untreated)
1340056	6720463M24Rik	0.00031	-1.75208
4780193	Aspm	0.00036	-1.59169
380520	Aurka	0.00017	-2.39294
7400215	Birc5	0.00019	-2.15796
2810612	Birc5	0.0003	-2.01431
1240446	Birc5	0.00047	-2.25534
5910528	Bub1b	0.00019	-2.06295
2190164	Ccnb1	6.56E-05	-3.06757
7550156	Ccnb1	0.00047	-3.03562
4610722	Cdc20	0.00012	-3.2905
4390228	Cdc20	0.00019	-2.93043
2320678	Cdc25c	3.38E-05	-1.81601
3830328	Cdc25c	5.71E-05	-2.0114
1050170	Cdca3	7.99E-05	-2.96694
4920148	Cdca3	0.00032	-1.91606
1500446	Cdca8	0.00038	-2.00116
7200519	Cenpa	2.32E-05	-3.48198
2710703	E130306D19Rik	3.77E-05	-1.94952
630634	Incenp	0.00016	-1.9118
4210246	Kif22	8.05E-05	-2.67197
1780543	Kif2c	0.00011	-2.61431
6940411	Pif1	8.06E-05	-2.43358
520427	Plk1	0.00012	-2.58357
780475	Prc1	0.00049	-2.65046
6620184	Spc25	0.00029	-1.94168

B The top 5-enriched predicted cellular function and canonical pathways, based on the 19 DEX-regulated genes.

Predicted Cellular Functions	p-value	Molecules
Cell Cycle	1.97E-17 - 3.87E-02	CDC25C, CDCA8, CDC20, PRC1, PLK1, AURKA, BUB1B, BIRC5, CCNB1, KIF22, ASPM, CENPA, KIF2C, INCENP
Cellular Assembly and Organization	1.94E-11 - 3.87E-02	CDC25C, CDCA8, CDC20, PRC1, PLK1, AURKA, BUB1B, BIRC5, PIF1, CCNB1, KIF22, CENPA, KIF2C, INCENP
DNA Replication, Recombination, and Repair	1.94E-11-3.78E-02	CDC25C, CDCA8, CDC20, PRC1, PLK1, AURKA, BUB1B, BIRC5, CCNB1 KIF22, CENPA, KIF2C, INCENP
Cellular Movement	2.49E-11-3.36E-02	CDC20, PRC1, PLK1, AURKA, BIRC5, CCNB1, INCENP
Cancer	1.22E-09-3.91E-02	CDC25C, CDCA8, CDC20, PRC1, PLK1, AURKA, BUB1B, BIRC5, CCNB1, KIF22, ASPM, CENPA, KIF2C, INCENP

Ingenuity Canonical Pathways	-log(p-value)	Molecules
Mitotic Roles of Polo-Like Kinase	8.64E+00	CDC25C, CDC20, PRC1, PLK1, CCNB1
Cell Cycle: G2/M DNA Damage Checkpoint Regulation	5.15E+00	CDC25C, PLK1, CCNB1
Role of CHK Proteins in Cell Cycle Checkpoint Control	2.99E+00	CDC25C, PLK1
ATM Signaling	2.91E+00	CDC25C, CCNB1
Hereditary Breast Cancer Signaling	2.35E+00	CDC25C, CCNB1